A&A 473, 437–444 (2007)
DOI: 10.1051/0004-6361:20077608

Astronomy & Astrophysics

Integrated spectral properties of 22 small angular diameter galactic open clusters⋆,⋆⋆

A. V. Ahumada[1,2], J. J. Clariá[1,2], and E. Bica[3]

[1] Observatorio Astronómico, Universidad Nacional de Córdoba, Laprida 854, 5000 Córdoba, Argentina
e-mail: andrea@oac.uncor.edu
[2] CONICET, Argentina
[3] Instituto de Física, Universidade Federal do Rio Grande do Sul, CP 15051, Porto Alegre 91501-970, RS, Brazil

Received 4 April 2007 / Accepted 6 July 2007

ABSTRACT

Aims. Flux-calibrated integrated spectra of a sample of 22 Galactic open clusters of small angular diameter are presented. With one exception (ESO 429-SC2), all objects have Galactic longitudes in the range $208° < l < 33°$. The spectra cover the range ≈3600−6800 Å, with a resolution of ≈14 Å. The properties of the present cluster sample are compared with those of well-studied clusters located in two 90° sectors, centred at $l = 257°$ and $l = 347°$. The dissolution rate of Galactic open clusters in these two sectors is examined.
Methods. Using the equivalent widths of the Balmer lines and comparing line intensities and continuum distribution of the cluster spectra with those of template cluster spectra with known properties, we derive both foreground reddening values and ages. Thus, we provide information independent of that determined through colour–magnitude diagrams.
Results. The derived $E(B-V)$ values for the whole sample vary from 0.0 in ESO 445-SC74 to 1.90 in Pismis 24, while the ages range from ∼3 Myr (NGC 6604 and BH 151) to ∼3.5 Gyr (Ruprecht 2). For six clusters (Dolidze 34, ESO 429-SC2, ESO 445-SC74, Ruprecht 2, BH 151 and Hogg 9) the foreground $E(B-V)$ colour excesses and ages are determined for the first time. The results obtained for the remaining clusters show, in general terms, good agreement with previous photometric results.
Conclusions. The age and reddening distributions of the present sample match those of known clusters in the two selected Galactic sectors. The present results would favour a major dissolution rate of star clusters in these two sectors. Two new solar-metallicity templates are defined corresponding to the age groups of (4−5) Myr and 30 Myr among those of Piatti et al. (2002, MNRAS, 335, 233). The Piatti et al. templates of 20 Myr and (3−4) Gyr are here redefined.

Key words. methods: observational – techniques: spectroscopic – open clusters and associations: general

1. Introduction

Open clusters have always played a prominent role in the delineation of the chemical as well as of the dynamical evolution of the Galactic disc (e.g., review by Friel 1995). This is due to the fact that their fundamental parameters may be determined more easily and more accurately than those for isolated stars. The young clusters have been used to determine the spiral arm structure, to investigate the processes of star formation and to constrain the initial luminosity and mass functions. On the other hand, intermediate-age and old Galactic open clusters are extremely useful as probes of both age and metallicity in the Galactic disk. Open clusters provide unique information on the metallicity gradients in the disc (e.g., Chen et al. 2003) and on the average stellar ages and radial velocities at different Galactic radii (e.g., Friel et al. 2002). They also provide information on the relationship between age and metallicity (e.g., Strobel 1991) and on the detailed morphology of the red giant region in the colour–magnitude diagram (CMD, e.g., Mermilliod et al. 2001). Research work, focused on any of the above-mentioned topics, requires observational data about the largest possible number of clusters spanning a wide age range.

Particularly, open clusters located towards the Galactic centre play an important role as they offer the possibility of tracing the structure and evolution of the inner disk. Many open clusters in this Galactic area, however, have not been studied in detail yet because they are affected by high interstellar absorption and/or strong field star contamination. A large number of these unstudied objects are definitely included in the approximately 60% of the 1632 open clusters known to exist in the Milky Way disc (Dias et al. 2002), which lack a CMD at present (Mermilliod & Paunzen 2003). Very little is known about all these objects, except the positions and the estimates of their angular sizes. Basic open cluster parameters such as reddening, distance and age have been mostly derived from CMDs and/or from photometric and kinematic studies of individual giants (e.g., Clariá et al. 2006). However, integrated spectra of small angular size open clusters have also proved to be a very useful tool to provide valuable independent information about their reddenings, ages and, in some cases, about their metallicities (e.g., Santos & Bica 1993). Efforts were made by Bica & Alloin (1986a,b), Bica (1988), Bica et al. (1990), Bonatto et al. (1995), Santos et al. (1995) and more recently by Piatti et al. (2002) to create reference spectra of star clusters in different spectral ranges and to define grids of their properties to be used as templates for different ages and metallicities in the study of composite stellar populations. Integrated spectra of small angular diameter Galactic

⋆ Based on observations made at Complejo Astronómico El Leoncito, which is operated under agreement between the Consejo Nacional de Investigaciones Científicas y Técnicas de la República Argentina (CONICET) and the National Universities of La Plata, Córdoba and San Juan, Argentina.

⋆⋆ Tables 2–4 and Appendix are only available in electronic form at http://www.aanda.org

Table 1. Cluster sample.

Cluster	l (°)	b (°)	α (h:m:s)	δ (°:′:″)	D (′)
Markarian 38, Biurakan 5	11.99	−0.94	18:15:16	−18:59:33	2
NGC 6604, Mel 197, Cr 374	18.26	1.69	18:18:06	−12:13:00	2
Dolidze 34	27.78	−0.01	18:42:03	−04:32:43	5
Berkeley 80	32.16	−1.25	18:54:21	−01:13:12	3
ESO 429-SC2	113.35	−28.19	07:33:23	−28:12:17	5
ESO 445-SC74	208.66	−31.96	13:54:43	−31:58:44	2.5
Bochum 2	212.30	−0.40	06:48:50	00:22:30	1.5
NGC 2311, Cr 123	217.73	−0.69	06:57:48	−04:36:42	6
NGC 2409, Bochum 4	232.48	0.77	07:31:37	−17:11:24	5
Ruprecht 2	238.78	−15.05	06:41:01	−29:33:00	3
Pismis 7, BH 43	259.03	2.00	08:41:54	−38:42:06	3
Hogg 9	288.84	0.69	10:58:22	−59:03:30	1
Hogg 10	290.80	0.10	11:10:42	−60:23:03	3
Basel 18	307.20	0.20	13:27:49	−62:18:47	3
Trumpler 21, Cr 274, BH 148	307.57	−0.30	13:32:14	−62:47:18	5
BH 151	308.69	0.60	13:40:12	−61:43:48	5
NGC 5281, Cr 276, Mel 120, BH 152	309.17	−0.70	13:46:37	−62:54:34	7
Lyngå 1	310.86	−0.38	14:00:02	−62:09:30	< 2
Pismis 20, BH 170	320.52	−1.21	15:15:23	−59:04:24	4
Hogg 22	338.55	−1.16	16:46:35	−47:04:57	1.2
NGC 6204, Cr 312, BH 196	338.59	−1.08	16:46:08	−47:00:44	5
Pismis 24, BH 227, NGC 6357	353.12	0.71	17:24:43	−34:12:23	2

open clusters are particularly important for high redshift studies, where integrated spectra of galaxies are often dominated by young stellar populations.

The present study is part of an ongoing systematic spectroscopic survey of Galactic open clusters located in different regions of the Milky Way. This survey is being undertaken at Complejo Astronómico El Leoncito (CASLEO) in San Juan (Argentina). Its first results dealt with 20 small angular diameter open clusters, most of which are located in the fourth Galactic quadrant (Ahumada et al. 2000, 2001). Out of these 20, 14 were previously unstudied objects. In this study we present flux-calibrated integrated and individual spectra of stars in the range ≈3800−6800 Å for 22 open clusters, five of which are projected close to the Galactic centre direction. Preliminary results for 5 out of the 22 clusters here analysed are presented in Ahumada et al. (2005). As an additional outcome of the present study, two new solar-metallicity templates were created among those of Piatti et al. (2002) and two others were redefined.

In Sect. 2 we present the cluster sample and the spectroscopic observations. The procedures employed to measure equivalent widths for Balmer absorption features, as well as to determine age and $E(B-V)$ reddening values, are described in Sect. 3. A comparison of the present results with those from other open clusters located in similar directions is presented in Sect. 4. In Sect. 5 we define two open-cluster templates among those of Piatti et al. (2002) and we redefine the 20 Myr and (3−4) Gyr templates from this spectral library. The final conclusions of the present study are summarised in Sect. 6. The analysis of the integrated and individual spectra of the selected clusters by the template matching and equivalent width methods is developed in Appendix A.

2. Spectroscopic data

2.1. Cluster sample and observations

The Milky Way, in the 90° sectors centred approximately at 0° and 270° of Galactic longitude, is particularly rich in open clusters, many of whose characteristics are still unknown. For this reason, we decided to carry out a spectroscopic survey of small angular diameter open clusters located preferably in these two Galactic sectors. All the objects were selected from the WEBDA Open Cluster Database (Mermilliod & Paunzen 2003), taking into account mainly their angular diameters (typically $D \leq 5'$) and their surface brightnesses. Small angular size open clusters are certainly the most suitable for carrying out integrated spectroscopic observations. This is because the cluster as well as the surrounding background sky regions extends along the whole slit. This angular size requirement results from, firstly, the fact that the cluster integrated spectrum must reflect the synthesis of its stellar populations and, secondly, the fact that when the reduction of the spectra is carried out, the subtraction of the sky, which is unavoidably overlapping the object, must be made.

In this study we selected 22 small angular diameter Galactic open clusters to allow good star sampling in the integrated spectra. Galactic and equatorial coordinates for the cluster sample are listed in Table 1, together with the angular sizes taken from Lyngå (1987), Lauberts (1982), Archinal & Hynes (2003, hereafter AH03) or estimated by ourselves through visual inspection on Digitized Sky Survey (DSS) images. Cluster designations in different catalogues are given in Table 1. The clusters are ordered according to their increasing Galactic longitude. Note that, except for ESO 429-SC2, the clusters analysed here have Galactic longitudes in the range $208° < l < 33°$.

The observations were carried out with the Jorge Sahade 2.15 m telescope at CASLEO over 11 nights between February 2000 and May 2003. In all the observing runs, we employed a CCD camera containing a Tektronix chip of 1024 × 1024 pixels attached to a REOSC spectrograph (simple mode), the size of each pixel being 24 μm × 24 μm. One pixel corresponds to 0.94″ on the sky. The slit was generally oriented east-west and the observations were performed by scanning the slit across the objects in the north-south direction to obtain a proper sampling of cluster stars. In some cases, however, the slit was appropriately rotated to include most of the cluster body. The number of times the objects crossed the slit during each scanning

depended basically on their angular sizes. Indeed, in the most compact clusters, each star within our area of interest crossed the slit a larger number of times than in the largest objects. By "area of interest" we mean either the cluster nuclei or else the regions of denser stellar concentration. In some cases, when one or more bright stars dominated the integrated light, individual spectra of those stars were obtained (Appendix A).

All exposures were made using a grating of 300 grooves mm^{-1} in six observing runs, producing an average dispersion in the observed region of ≈140 Å/mm (3.46 Å/pixel). The CCD operated with a gain of 1.98 e^-/ADU and a readout noise of 7.4 e^-/ADU. The spectral coverage was ≈3800−6800 Å. The total field along the slit was 4.7′, which allowed us to sample regions of background sky in most clusters. The seeing during the nights was typically 1.5″−3.0″. The slit width was 400 μ (∼4.2″ in the sky) resulting in a resolution [full width at half-maximum (*FWHM*)] of ∼14 Å, as deduced from the Cu-Ar-Ne comparison lamp lines. The standard stars LTT 2415, LTT 3864, CD -32°9927, LTT 6248, EG 274, LTT 7379 and LTT 7987 from the list of Stone & Baldwin (1983) were observed for flux calibrations. Bias, dome and twilight sky flats were taken and employed in the reductions.

The journal of observations is provided in Table 2 (online material), whose columns give in succession: (1) cluster designation, (2) date of observation, (3) number of exposures and duration in seconds, (4) *FWHM* in arcseconds determined by the seeing during observation, (5) total area of the cluster scanned in our observations, and (6) signal-to-noise (S/N) ratio per Angstrom measured in the (5000−5500 Å) spectral interval in regions free from emission and/or absorption lines of the final spectra. As expected, the S/N ratio corresponding to the sum of several spectra was always larger than that of the corresponding individual spectra.

The reduction of the spectra was carried out with the *IRAF*[1] software package at the Observatorio Astronómico de la Universidad Nacional de Córdoba (Argentina) according standard procedures. Summing up, we subtracted the bias and used flat-field frames – previously combined – to correct the frames for high and low spatial frequency variations. Background sky subtractions were then performed using pixel rows from the same frame after removing cosmic rays from the background sky regions, taking care that no significant background sky residuals were present on the resulting spectra. The cluster spectra were extracted along the slit according to the cluster size and available flux. For larger objects, we scanned the slit along the north-south direction in order to better sample the cluster stellar population. Some clusters actually present angular diameters larger than the total field along the slit. The spectra were obtained in these cases by scanning first one portion of the main body of the cluster from which the background sky was subtracted. We then obtained the spectrum of the remaining portion of the cluster from which we also subtracted the background sky. The final spectrum results from the sum of the two mentioned spectra. The resulting spatial coverages are given in Table 2. Spectra were then wavelength-calibrated by fitting observed Cu-Ar-Ne comparison lamp spectra with template spectra. The rms errors involved in these calibrations are typically 0.50 Å (0.14 pixel). Finally, we made atmospheric extinction corrections to the cluster spectra according to the site coefficients given by Minniti et al. (1989). Flux calibrations were performed using the observed standard stars. The spectra obtained in different runs were averaged by weighting them according to their S/N ratios.

[1] *IRAF* is distributed by the National Optical Astronomy Observatories, which is operated by the Association of Universities for Research in Astronomy, Inc., under contract with the National Science Foundation.

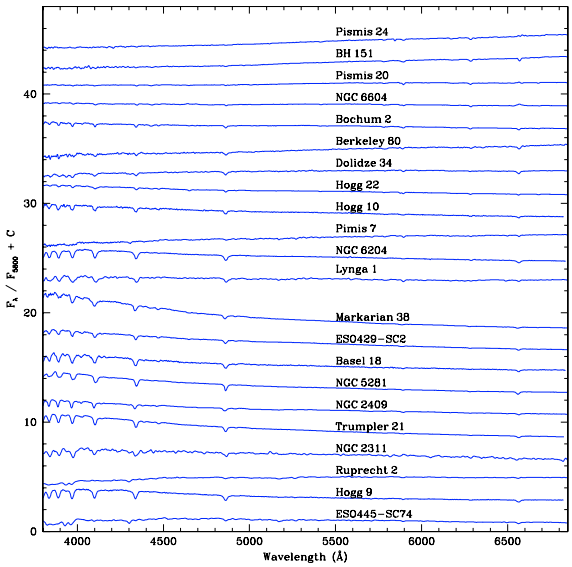

Fig. 1. Observed integrated spectra of the sample clusters. Spectra are in relative F_λ units normalised at ≈5800 Å. Constants have been added to the spectra, except for the bottom one.

Figure 1 shows the resulting flux-calibrated integrated spectra of the 22 observed clusters. Such spectra are given in relative F_λ units normalised at $\lambda \approx 5800$ Å and have been ordered from bottom to top according to their increasing reddening. Constants have been added to the spectra, except for the bottom one, to allow for comparison. All observed spectra are available upon request to the first author. Although the spectral lines and different slopes of the continuum energy distributions in Fig. 1 are primarily the result of age effects, the steepest spectra in the upper part of Fig. 1 reveal strong dust absorption effects. They correspond to the most reddened open clusters BH 151 and Pismis 24, which are discussed in Appendix A. Note that while some field star contamination may be expected in the observed spectra, only bright field stars could affect the spectra significantly. In those clusters showing bright stars in their fields, we obtained individual spectra of those stars and different extractions were considered in the discussion of each cluster (Appendix A).

2.2. Equivalent width measurements

Equivalent widths (EWs) in the observed spectra are unaffected by reddening and, consequently, they reflect intrinsic stellar atmospheric properties. Before measuring EWs, the spectra were normalised at approximately 5800 Å. The flux normalisation at this wavelength is meant to represent the continuum flux around 5800 Å, thus avoiding spectral lines eventually present. In practice, the spectral region around 5800 Å (≈20 Å wide) is examined and the normalization is applied to a nearby wavelength representative of the continuum flux. Spectral fluxes at 3860 Å, 4020 Å, 4150 Å, 4570 Å, 4834 Å, 4914 Å and 6630 Å were used as guidelines to define the continuum according to Bica & Alloin (1986a). The EWs of the four primary H Balmer lines were measured within the spectral windows defined by Bica & Alloin (1986a) using the SPEED program (Schmidt 1988) for the spectra analyses. Typical errors of ≈10% on individual EW

measurements were the result of tracing slightly different continua. The results of the measurements are shown in Table 3 (online material), where the EWs are given in Angstrom units (Å). Only the first cluster designation is listed in the first column of Table 3.

3. Reddening and age determination

Age and foreground reddening $E(B-V)$ values of the selected clusters were simultaneously derived by means of the template matching method described by Santos & Bica (1993). This was done by achieving the best possible match between the continuum and lines of the analysed cluster integrated spectrum and those of a template integrated spectrum with known properties. In this process, we selected from the available template spectra, those which minimise the flux residuals, calculated as the normalised difference (cluster – template)/cluster. Note that differences between cluster and template spectra are expected to be found due to variations in the stellar content of the cluster, such as the presence of a relatively bright star with particular spectral features or contamination of a field star close to the direction of the cluster. To apply the template matching method, a direct reddening-independent age estimate was firstly obtained from EWs of the Balmer absorption lines in each spectrum. This was done by interpolating the EW values in the age calibration of Bica & Alloin (1986b, their Table II). Notice that the Balmer lines reach their peak value at t (age) $\approx$ 500 Myr, while spectra of intermediate-age clusters have strong metallic lines in the blue range like K CaII. Based on this age first estimate, we selected among the templates of Piatti et al.'s (2002) database, a subset of templates to compare with the observed spectrum. This selection allowed us to constrain our search of the most appropriate template since those selected are within a certain age range. We note that the Balmer age is a first approach, which enables us to deal with a smaller number of templates that in Piatti et al. (2002). The final age determination was made in a second step by varying reddening and template until the best match of continuum, Balmer and metal lines to that of the best fitting template was obtained. To perform reddening corrections, we used the normal reddening law (Seaton 1979), the relation $A_v = 3E(B-V)$ and the SPEED program (Schmidt 1988). The results are shown in Figs. A.1 to A.37 (Appendix A, online material).

Table 4 (online material) shows the age and foreground reddening values obtained from the template matching method for the present cluster sample. The columns give in succession: the first cluster designation, the derived foreground reddening $E(B-V)$ value and its estimated uncertainty, the approximate age inferred from the Balmer lines, the age of the Piatti et al. (2002) template with which the best match was obtained and the age finally adopted for the cluster. The last two columns of Table 4 list ages taken from the literature (when available) and the corresponding references. Note that the uncertainty in the adopted reddening $E(B-V)$ values represents the minimum reddening variation needed to distinguish the cluster spectrum from that of the matching template. We estimated this uncertainty by comparing the residual fluxes left after using different reddenings. Table 4 shows that these uncertainties vary from 0.02 to 0.05 mag. If the age assignment were to be shifted by one template type, the uncertainty mentioned above would be only slightly larger.

To apply the template matching procedure, all the templates from the open-cluster integrated spectral library of Piatti et al. (2002) were found to be useful in this work. These templates depend primarily on age, the metallicity effects being practically negligible in the spectral and age ranges considered here, except perhaps for the clusters older than 1−2 Gyr.

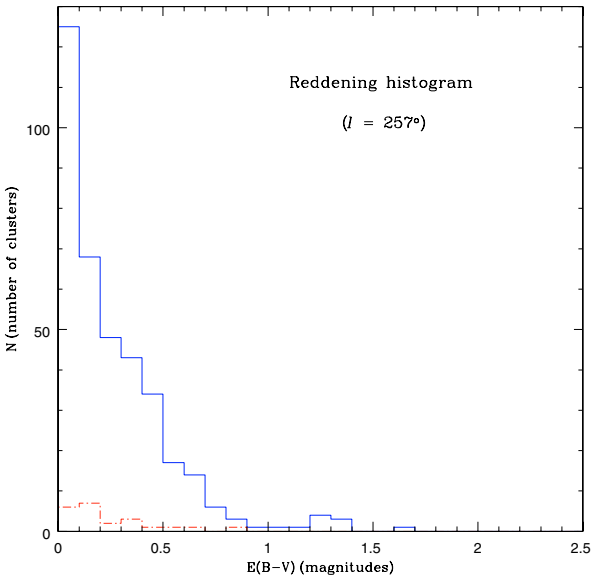

Fig. 2. Reddening histograms in the 90° Galactic sector centred at l = 257°. The histogram corresponding to 365 known open clusters with $E(B-V) < 2.5$ is shown in solid lines. The dashed lines show the histogram for the 42 open clusters within $E(B-V)$ intervals of 0.1 mag wide.

4. Comparison with known open clusters located in the same Galactic sectors

The present cluster sample, together with those previously analised using the same technique (Ahumada et al. 2000, 2001), represents a statistically meaningful sample of 42 open clusters of the Galactic disc. We considered it interesting to compare the parameters determined via integrated spectroscopy for these 42 clusters with those of well-known clusters located in similar regions of the Galactic disc. We believe that it is important to compare this statistically meaningful cluster sample with open clusters already studied in the literature in similar disc regions because the current sample deals with relatively faint clusters, on average fainter than more prominent objects which have reported CMD studies in the literature. Clusters such as the present ones are numerous in catalogues and are likely to be the most frequent kind of young disc targets for CMD studies in the coming years.

With the exception of ESO 429-SC2, all the clusters studied spectroscopically almost lie within two 90° Galactic sectors centred respectively at l = 257° and l = 347°. Note that these two Galactic longitudes are very close to l = 270° and l = 0° (Galactic centre), respectively. Twenty-two clusters out of the 42 are located in the first Galactic sector, while the remaining 19 lie within the second sector. With the aim of comparing the reddening and age values of the 42 clusters with those of known open clusters located in these two selected sectors, we used the WEBDA Open Cluster Database (Mermilliod & Paunzen 2003). This database offers a periodically updated compilation of the fundamental parameters of open clusters to search clusters with well determined ages and $E(B-V)$ colour excesses.

We show in Fig. 2 the reddening histogram for the Galactic sector centred at l = 257°, which includes 365 open clusters with $E(B-V) < 2.5$ (solid lines). We show in dashed lines the

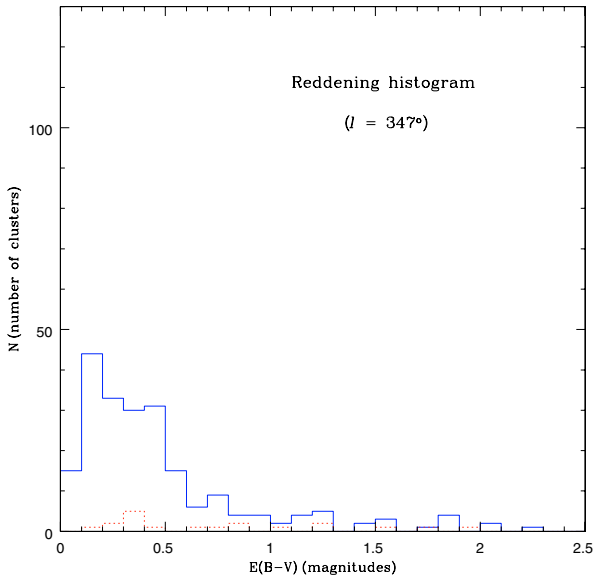

Fig. 3. Reddening histograms in the 90° Galactic sector centred at l = 347°. Symbols as in Fig. 2.

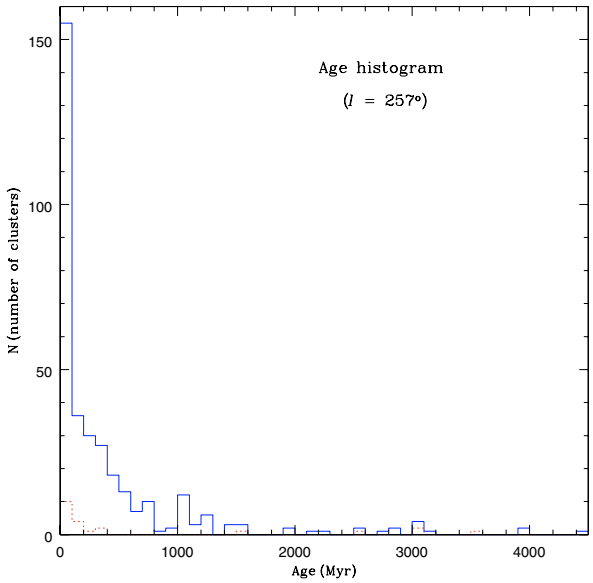

Fig. 4. Age histograms in the 90° Galactic sector centred at l = 257°. The histogram corresponding to the WEBDA open cluster younger than 4 Gyr is shown in solid lines. The histogram for the 42 open-cluster sample is shown in dashed lines.

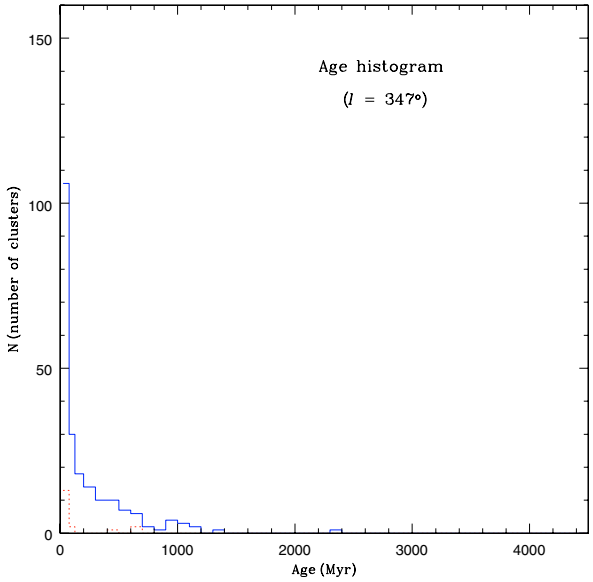

Fig. 5. Age histograms in the 90° Galactic sector centred at l = 347°. Symbols as in Fig. 3.

histogram for the 42 open clusters within $E(B-V)$ intervals of 0.1 mag wide. The distribution of the reddening values of the 42 open clusters certainly resembles the typical reddening distribution in this Milky Way zone. Indeed, in Fig. 2, 19 out of the 22 spectroscopically studied objects show reddenings between 0.0 and 0.5. This is precisely the reddening interval where the cluster colour excesses reach their peak value. Besides, note that none of the studied clusters exceeds the maximum reddening value for this sector.

Similar histograms are presented in Fig. 3 for the clusters of the sector centred at l = 347°. The solid histogram includes 215 open clusters with known parameters from the WEBDA database. As in the sector centred at l = 257°, the distribution of $E(B-V)$ colour excesses of the 19 open clusters examined here is typical of the sector, or the distribution that could be expected according to existing data for this region of the Milky Way. None of the studied clusters, in fact, present an $E(B-V)$ value larger than 2.0 mag. In addition, 11 out of the 19 clusters lie in a region of the histogram where reddening values are more frequent.

The age histograms for the two Galactic sectors are shown in Figs. 4 and 5. The solid histograms were built by selecting from WEBDA all the clusters whose ages are known, except for those clusters older than 4 Gyr since only six objects from WEBDA exceed this value. We counted clusters within age intervals of 100 Myr. The histograms for the 42 open-cluster sample are shown in dashed lines. The Galactic sector centred at l = 257° (Fig. 4) is found to have 17 of the clusters studied here (77%), which correspond to the most frequent type, i.e., very young or moderately young open clusters, aged under 400 Myr. Only four out of the 22 clusters studied in this sector (Berkeley 75, Ruprecht 2, ESO 445-SC74 and Pismis 7), seem to be part of a fairly unusual sample of intermediate-age or old open clusters. A similar feature can be observed in Fig. 5 for clusters in the range 302° < l < 32°. In this case, 84% of the studied clusters are younger than 200 Myr, precisely located in the histogram region where the age distribution is at its peak value. As the age increases, the cluster frequency decreases remarkably in both Galactic sectors. The age distribution must reflect the formation/dissoluton rates of star clusters, perhaps biased by observational constraints. Our cluster sample suggests, however, that the age distribution will not change a lot in the future when new faint clusters are observed. As an observational bias seems improbable, the age histograms must intrinsically indicate a real drop. The results of the current study tend to support the conclusion that unless major star-forming events had occurred in the Galactic disc in the last 100 Myr or so, the present results would favour a major dissolution rate of star clusters in the two Galactic sectors examined.

5. New open-cluster template spectra

As shown in Appendix A, some clusters present intermediate ages among the templates defined by Piatti et al. (2002). Since the integrated spectra of these intermediate age objects exhibit, in general terms, a good S/N ratio, we averaged them in order

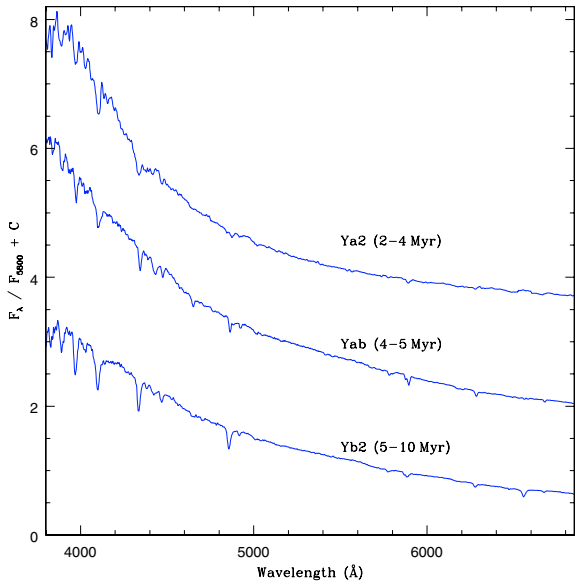

Fig. 6. Ya2 template spectrum of (2−4) Myr (*top*), Yb2 template spectrum of (5−10) Myr (*bottom*) and the new Yab template spectrum of (4−5) Myr (*middle*) defined in the current study.

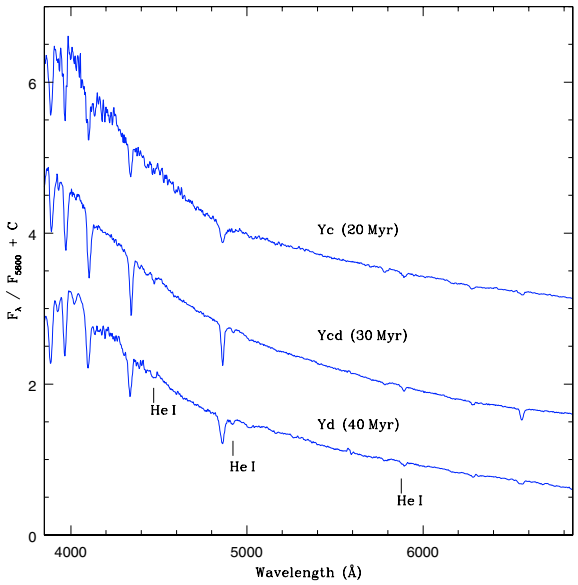

Fig. 7. Yc template spectrum of 20 Myr (*top*), Yd template spectrum of 40 Myr (*bottom*) and the new redefined Ycd template spectrum of 30 Myr (*middle*).

to define new open-cluster templates and to improve the temporal resolution of Piatti et al. (2002) library. The individual spectra which originated each new "intermediate" template, fulfil the requirements of having both the same spectral continuum distribution and the same or quite similar absorption lines. Thus, two new templates were defined between (2−4) and (5−10) Myr and between 20 and 40 Myr, respectively.

5.1. The Yab template of (4–5) Myr

To define a new open-cluster template of an intermediate age between (2−4) and (5−10) Myr, the reddening-corrected spectra of Pismis 20 and Hogg 22 were combined. As mentioned in Appendix A.19, the best match of the reddening-corrected Pismis 20 spectrum was obtained with the template Ya3 of (2−4) Myr. There are, however, some spectral features in Pismis 20 which are not present in the Ya3 template, which indicate that this cluster must be a little older than the template. It is for this reason that in Appendix A.19 we made an alternative comparison with the (5−10) Myr template. Vázquez et al. (1995) photometrically determined for Pismis 20 $E(B-V) = 1.24$ and an age of 5 Myr. Turner (1996), in turn, obtained a very similar colour excess, namely $E(B-V) = 1.28$. The results of the integrated spectroscopy are fully compatible with those derived in the above-mentioned studies. We adopted for Pismis 20 an intermediate age between the two templates, i.e., 5 ± 1 Myr. The age of 4.5 ± 2.0 Myr assigned to Hogg 22 (Table 4) is also an intermediate age between the templates of (2−4) and (5−10) Myr. Both the spectroscopic reddening and age of Hogg 22 agree with the values reported by Moffat & Vogt (1973, hereafter MV73) and Kharchenko et al. (2005).

Templates Ya2 of (2−4) Myr (top), Yb2 of (5−10) Myr (bottom) and the new Yab template of (4−5) Myr defined here (middle) are displayed in Fig. 6. Note how the Balmer line depths gradually increase from the youngest to the oldest template, whereas in the new Yab template the Balmer lines exhibit an intermediate depth between both spectra. The younger the object, the larger the flux emitted in the blue-violet spectral region. This characteristic proves that the Yab template's age is slightly closer to that of the (2−4) Myr template than to the (5−10) Myr one. Therefore, we adopted an age of (4−5) Myr for the Yab intermediate template.

5.2. The Ycd template of 30 Myr

After analysing the reddening-corrected spectra of Hogg 10, Trumpler 21 and NGC 5281 (Appendix A), we concluded that these three objects are approximately 30 Myr old. Given the fact that these clusters' spectra have a good S/N ratio, we combined them to define a new Ycd template of 30 Myr, which is in between Yc (20 Myr) and Yd (40 Myr) templates from Piatti et al. (2002). The Ycd template, together with the Yc and Yd templates, are shown in Fig. 7. Although in this case a gradual variation in the Balmer line depths is not visible, the intermediate characteristics of the new template are evident in the blue-violet continuum distribution (4000 Å break) as well as in the gradual variation of HeI 4471 Å, 4921 Å and 5875 Å lines. This is probably due to the contribution of the supergiant star HD 119699 of NGC 5281.

5.3. Redefinition of the Yc template

Piatti et al. (2002) created the Yc template of 20 Myr by averaging the reddening-corrected spectra of Hogg 15, Ruprecht 119, BH 217, NGC 6318 and BH 245. Nevertheless, as can be seen in Fig. 5 from Piatti et al. (2002), the quality of this template presents a contrast with that of the other moderately young templates of the same spectral library. A careful examination of the 5 individual spectra used to define the Yc template of 20 Myr demonstrates that the somewhat poorer quality of this template – especially in the blue-violet spectral region – is due to the low S/N ratio of the spectra of BH 245 and NGC 6318 obtained by Piatti et al. (2000). Although the integrated spectrum of Ruprecht 119 has a good S/N ratio, we chose not to include it to redefine the Yc template for two reasons: (1) The Ruprecht 119 spectrum exhibits Hα in emission. (2) The Hβ line in the Ruprecht 119 spectrum appears to be unusually broadened

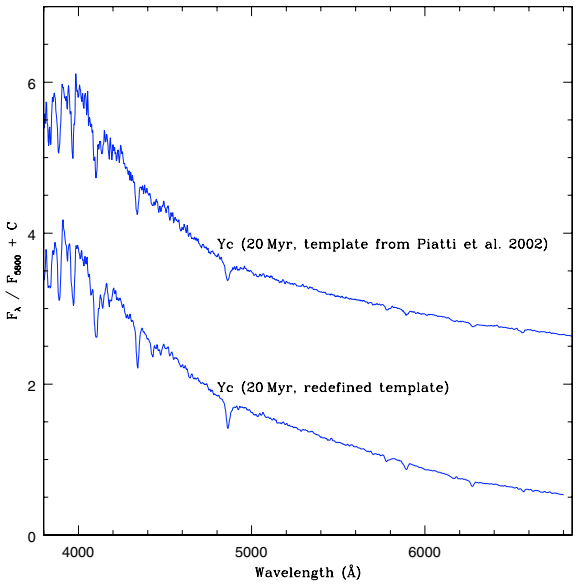

Fig. 8. Comparison of the Piatti et al. (2002) Yc template spectrum of 20 Myr (*top*) with the new Yc template spectrum of 20 Myr (*bottom*) redefined in the current study.

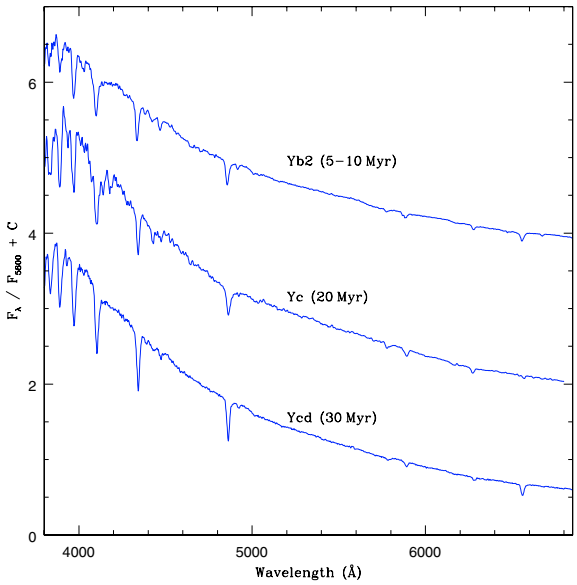

Fig. 9. *From top to bottom*: the Yb2 template spectrum of (5−10) Myr, the redefined Yc template spectrum of 20 Myr and the new Ycd template spectrum of 30 Myr defined in the current study.

if compared with the same line in other spectra of about the same age. Furthermore, Piatti et al. (2005) recently found out that the age of NGC 6318 is ∼8 times older than the age determined from the poorer quality integrated spectrum.

In Fig. 8 we compare Piatti et al.'s (2002) Yc template of 20 Myr (top), which was defined by combining the spectra of the 5 above-mentioned clusters, with the new Yc template of 20 Myr (bottom). The latter results from the combination of the spectra of only Hogg 15 and BH 217. It is worth noting that some spectral features practically indistinguishable in the original Yc template can now be clearly seen in the Yc template redefined here. Also note how the wavelength in which the maximum flux value is reached exhibits a slight change. The temporal sequence made up of the Yb2 template of (5−10) Myr (top), of the redefined Yc template of 20 Myr (middle) and the new Ycd template of 30 Myr (bottom), is shown in Fig. 9. In the same sequence, the gradual variation of the intensity of the Balmer lines as the cluster age increases is clearly seen. At the same time, in the region where wavelengths are shorter than 4600 Å a slighter variation in the spectra slopes can be observed.

5.4. Redefinition of the Ib template

The Ib template of (3−4) Gyr from Piatti et al. (2002) also does not present a good S/N ratio, mainly in the blue-violet spectral region. This template was defined by averaging the reddening-corrected spectra of NGC 2158, Berkeley 75, ESO 93-SC8 and NGC 6253. It is evident that the low S/N ratio of the spectra of NGC 2158 and Berkeley 75 reduces the quality of the Ib template. Moreover, in Appendix A.10 we concluded that Ruprecht 2 is (3−4) Gyr old. Therefore, we decided to redefine Ib template of (3−4) Gyr by combining the reddening-corrected spectra of ESO 93-SC8, NGC 6253 and Ruprecht 2, all of which exhibit a good S/N ratio. The redefined Ib template is shown in Fig. 10 (bottom). The redefined Ib template is remarkably improved, particularly for $\lambda < 4300$ Å, if compared with the original Ib template. The TiO bands visible in $\lambda \sim (6100-6400)$ Å are due to the red giant component of NGC 6253 (Piatti et al. 1998).

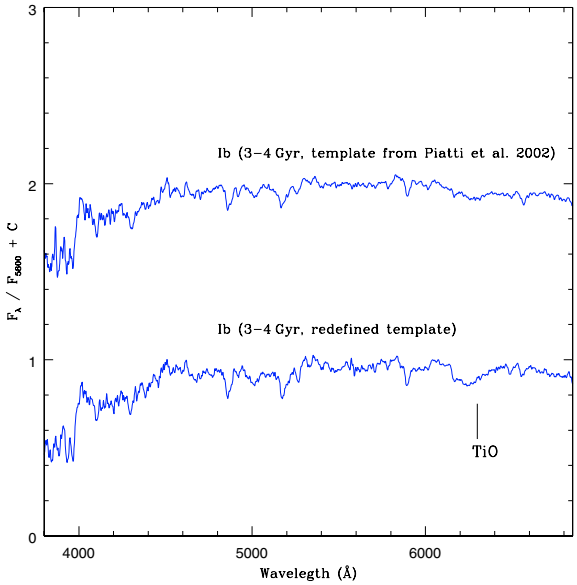

Fig. 10. Comparison of the Piatti et al. (2002) Ib template spectrum of (3−4) Gyr (*top*) with the redefined Ib template spectrum (*bottom*).

6. Concluding remarks

In the present paper we studied a sample of 22 small angular size Galactic open clusters by means of integrated spectroscopy in the optical range. With one exception (ESO 429-SC2), the remaining objects are located within the range $208° < l < 33°$. Six out of the 22 studied clusters have been not previously studied so that the fundamental parameters determined in the current study are the first of their kind. For the remaining clusters, the parameters determined here exhibit, in general terms, good agreement with those derived in previous photometric studies, Pismis 7 being an exception. The age estimated here for this cluster (∼3 Gyr), is considerably older than that obtained from *CCD BVRI* photometry. In all cases, the ages and foreground interstellar reddening values were determined using equivalent widths of the Balmer absorption lines and comparing the

observed spectra with template spectra. The present cluster sample complements previous ones (Ahumada et al. 2000, 2001), in an effort to gather a spectral library with several clusters per age interval.

The $E(B-V)$ colour excesses derived for the whole sample range from 0.0 in ESO 445-SC74 to 1.90 in Pismis 24, while the ages vary from ∼3 Myr in NGC 6604 and BH 151 to ∼3.5 Gyr in Ruprecht 2. Six of the observed clusters proved to be very young with ages about or under 5 Myr, whereas ten clusters can be considered moderately young with ages between 7.5 and 300 Myr. Two objects (Dolidze 34 and Berkeley 80) are Hyades-like age clusters ($t \sim 600$ Myr) and only three (ESO 445-SC74, Ruprecht 2 and Pismis 7) are either intermediate-age or definitely old clusters with ages similar to or older than 2.5 Gyr. A more detailed study of these three clusters is recommended.

The present cluster sample complements that of 20 open clusters previously studied by Ahumada et al. (2000, 2001) using the same technique. We have compared the properties of the whole sample (42 clusters) with those of open clusters located in two 90° sectors, centred at $l = 257°$ and $l = 347°$, respectively, already studied in the literature. Unless major star-forming events took place in the Galactic disc in the last 100 Myr or so, it seems evident that this comparison supports the conclusion that there was an important dissolution rate of star clusters in the above-mentioned Galactic sectors.

Among some previously-defined consecutive spectral groups, two new open-cluster template spectra of intermediate ages are here created. This implies a refinement of the spectral library of Piatti et al. (2002) and an improvement of its temporal resolution. Finally, the open-cluster templates of 20 Myr and of 3.5 Gyr of Piatti et al. (2002) were redefined using only spectra of high S/N ratio, improving their quality.

Acknowledgements. We thank the staff and personnel at CASLEO for hospitality and assistance during the observations. The authors acknowledge use of the *CCD* and data acquisition system supported under US National Science Foundation grant AST-90-15827 to R. M. Rich. We appreciate the valuable comments and suggestions of the referee, Dr. Ricardo Schiavon, which helped us to improve the manuscript. We gratefully acknowledge financial support from the Argentinian institutions CONICET and SECyT (Universidad Nacional de Córdoba) and the Brazilian institutions CNPq and FINEP. We have used images from the Digitized Sky Survey (produced at the Space Telescope Science Institute under US Government grant NAG W-2166) by means of the Canadian Astronomy Data Centre (CADC) interface. This research has made use of the SIMBAD database, operated at CDS, Strasbourg, France; also the WEBDA database, operated at the Institute for Astronomy of the University of Vienna, and the NASA's Astrophysics Data.

References

Ahumada, J. A. 2005, Astron. Nachr., 326, 3
Ahumada, A. V., Clariá, J. J., Bica, E., & Piatti, A. E. 2000, A&A, 141, 79
Ahumada, A. V., Clariá, J. J., Bica, E., Dutra, C. M., & Torres, M. C. 2001, A&A, 377, 845
Ahumada, A. V., Clariá, J. J., & Bica, E. 2005, Bol. Asoc. Arg. Astron., 48, 140
Archinal, B. A., & Hynes, S. J. 2003, Star Clusters (Willman-Bell, Inc.) (AH03)
Barbon, R., Carraro, G., Munari, U., Zwitter, T., & Tomasella, L. 2000, A&AS, 144, 451
Bica, E. 1988, A&A, 195, 76
Bica, E., & Alloin, D. 1986a, A&A, 162, 21
Bica, E., & Alloin, D. 1986b, A&AS, 66, 171
Bica, E., Alloin, D., & Santos Jr, J. F. C. 1990, A&A, 235, 103
Bonatto, C., Bica, E., & Alloin, D. 1995, A&AS, 112, 71
Carraro, G., Janes, K. A., & Eastman, J. D. 2005, MNRAS, 364, 179
Carraro, G., & Munari, U. 2004, MNRAS, 347, 625
Chen, L., Hou, J. L., & Wang, J. J. 2003, AJ, 125, 1397
Clariá, J. J. 1976, AJ, 81, 155
Clariá, J. J., Lapasset, E., & Minniti, D. 1989, A&AS, 78, 363
Clariá, J. J., Piatti, A. E., Mermilliod, J.-C., & Parisi, M. C. 2006, A&A, 453, 91
Collinder, P. 1931, Medd. Lunds. Astron. Obs., 2
Dias, W., Alessi, B. S., Moitinho, A., & Lepine, J. R. D. 2002, A&AS, 141, 371
Dolidze, M. V. 1961, On the star cluster near γ Cyg., Astr. Cirk., 223, 11
Dutra, C. M., Bica, E., Soares, J., & Barbuy, B. 2003, A&A, 400, 533
Fenkart, R. P., Binggeli, G., Good, D., Jenni, L., & Tschumi, A. 1977, A&AS, 30, 307
Forbes, D., & Dupuy, D. L. 1978, AJ, 83, 266
Friel, E. D. 1995, ARA&A, 33, 381
Friel, E. D., Janes, K. A., Tavarez, M., et al. 2002, AJ, 124, 2693
Giorgi, E. E., Baume, G., Vázquez, R. A., & Feinstein, A. 2001, Rev. Mex. Astron. Astrofis., 37, 15
Grubissich, C., & Becker, W. 1980, A&AS, 40, 367
Hogg, A. R. 1965a, Mem. Mount Stromlo, 17
Hogg, A. R. 1965b, PASP, 77, 440
Houck, N., & Cowley, A. P. 1975, University of Michigan Catalogue of Two-Dimensional Spectral Types for the HD Stars, Vol. I
Iskurzdajan, S. G. 1959, Proc. of Armeny Academy of Sciences, 29, 5
Kharchenko, N. V., Piskunov, A. E., Roeser, S., Schilbach, E., & Scholz, R. D. 2005, A&A, 438, 1163
Lauberts, A. 1982, The ESO/Uppsala Survery of the ESO (B) Atlas, European Southern Observatory, Garching
Lundstrom, I., & Stenholm, B. 1984, A&AS, 58, 163
Lyngå, G. 1965, Lund Medd. Astron. Obs., SII, 142
Lyngå, G. 1987, Catalogue of Open Cluster Data, Strasbourg, Centre de Données Stellaires
Markarian, B. E. 1951, On the classification of open (galactic) clusters. II. Preliminary list of O-type star clusters, Soob. Biurakan Obs., 9
Massey, P., & Johnson, J. 1993, AJ, 105, 980
Massey, P., DeGioia-Eastwood, K., & Waterhouse, E. 2001, AJ, 121, 1050
Melotte, P. J. 1915, Mem. RAS, 60, 181
Mermilliod, J.-C., & Paunzen, E. 2003, A&A, 410, 511
Mermilliod, J.-C., Clariá, J. J., Andersen, J., Piatti, A. E., & Mayor, M. 2001, A&A, 375, 30
Minniti, D., Clariá, J. J., & Gómez, M. 1989, Ap&SS, 158, 9
Moffat, A. F. J., & Vogt, N. 1973, A&A, 10, 135 (MV73)
Moffat, A. F. J., & Vogt, N. 1975a, A&AS, 20, 85
Moffat, A. F. J., & Vogt, N. 1975b, A&AS, 20, 125
Moffat, A. F. J., & Vogt, N. 1975c, A&AS, 20, 155
Munari, U., & Carraro, G. 1995, MNRAS, 277, 1269
Pavani, D. B., Bica, E., Ahumada, A. V., & Clariá, J. J. 2003, A&A, 399, 113
Peterson, C. J., & Fitzgerald, M. P. 1988, MNRAS, 235, 1439
Piatti, A. E., Bica, E., & Clariá, J. J. 1998, A&AS, 127, 243
Piatti, A. E., Bica, E., & Clariá, J. J. 2000, A&A, 362, 959
Piatti, A. E., Bica, E., Clariá, J. J., Santos Jr, J. F. C., & Ahumada, A. V. 2002, MNRAS, 335, 233
Piatti, A. E., Clariá, J. J., & Ahumada, A. V. 2005, PASP, 117, 22
Pismis, P. 1959, Bol. Obs. Tonantzintla y Tacubaya, 18, 37
Rodgers, A. W., Campbell, C., & Whiteoak, J. B. 1960, MNRAS, 121, 103
Ruprecht, J. 1966, Bull. Astron. Czechoslovakia, 17, 33
Sagar, R., Munari, U., & de Boer, K. S. 2001, MNRAS, 327, 23
Sanner, J., Brunzedorf, J., Will, J.-M., & Geffert, M. 2001, A&A, 369, 511
Santos Jr, J. F. C., & Bica, E. 1993, MNRAS, 260, 915
Santos Jr, J. F. C., Bica, E., Clariá, J. J., et al. 1995, MNRAS, 276, 1155
Schmidt, A. 1988, SPEED User's Manual, Univ. Federal do Santa María, Brazil
Seaton, M. J. 1979, MNRAS, 187, 73
Silva, D. R., & Cornell, M. E. 1992, ApJS, 81, 865 (SC92)
Steilin, U. 1968, Z. Astrophys., 69, 276
Stephenson, C. B., & Sanduleak, N. 1971, Publ. Warner & Swasey Obs. 1, No. 1
Stone, R. P. S., & Baldwin, J. A. 1983, MNRAS, 204, 347
Strobel, A. 1991, ApJ, 376, 204
Trumpler, R. J. 1930, Lick Obs. Bull., 14, 154
Turbide, L., & Moffat, A. F. J. 1993, AJ, 105, 1831
Turner, D. G. 1996, AJ, 111, 828
van den Bergh, S., & Hagen, G. L. 1975, AJ, 80, 11
van der Hucht, K. A., Conti, P. S., Lundstrom, I., & Stenholm, B. 1981, Space Sci. Rev., 28, 227
Vázquez, R. A., Will, J.-M., Prado, P., & Feinstein, A. 1995, A&AS, 111, 85
Vázquez, R. A., Giorgi, E. E., Brusaco, M. A., Baume, G., & Solivella, G. 2003, RMAA, 39, 89
Vogt, N., & Moffat, A. F. J. 1975, A&A, 39, 477
Walborn, N. 1973, AJ, 78, 1067
Walborn, N. 1994, in The MK Process at 50 years, ed. C. J. Corbally, R. O. Gray, & R. F. Garrison (San Francisco: ASP), ASP Conf. Ser., 60, 84
Whiteoak, J. B. 1963, MNRAS, 125, 105

Online Material

Table 2. Journal of observations.

Cluster	Date (UT)	Exposure Time (s)	*FWHM* (″)	AREA (“×”)	*S*/*N*
Markarian 38	5/25/03	2 × 300	2.7	2.5 × 2.5	32
		2 × 60			
		1 × 1200			
NGC 6604	5/21/01	3 × 900	5.4	4 × 4	50
Dolidze 34	5/08/02	3 × 600	2.5	4 × 2	34
Berkeley 80	5/08/01	4 × 900	4.5	3.5 × 2.5	25
	5/08/02	1 × 1200	3.2		
	5/09/02	3 × 1200	2.6		
ESO 429-SC2	11/21/01	2 × 900	3.6	3 × 2	25
ESO 445-SC74	5/09/02	3 × 1200	2.7	2 × 2	35
Bochum 2	11/21/01	2 × 900	3.0	2 × 1.5	26
NGC 2311	12/15/01	2 × 900	3.1	4 × 3	19
NGC 2409	12/15/01	3 × 900	4.5	3 × 3	41
Ruprecht 2	12/15/01	2 × 900	2.7	2 × 3	36
Pismis 7	2/07/00	4 × 900	2.6	3 × 2	31
	5/20/01	3 × 900	3.6		
	5/21/01	2 × 900	4.7		
Hogg 9	5/21/01	2 × 900	3.6	1.5 × 1	34
	5/21/03	2 × 1200	3.0		
Hogg 10	5/21/01	4 × 900	4.5	2.5 × 2	45
	5/25/03	2 × 900	2.5		
Basel 18	5/24/03	6 × 600	2.7	3 × 6	33
Trumpler 21	5/27/03	2 × 1800	2.7	4 × 4	26
BH 151	2/07/00	4 × 900	2.7	1.5 × 2.5	27
	5/20/01	4 × 900	3.6		
	5/08/02	3 × 1200	2.0		
NGC 5281	5/21/01	3 × 900	5.0	3 × 5	35
Lyngå 1	5/20/01	4 × 900	3.0	2 × 4	26
Pismis 20	5/20/01	3 × 900	3.8	2.5 × 2	40
Hogg 22	5/21/01	2 × 900	5.1	6 × 3	39
	5/08/02	2 × 300	2.7		
NGC 6204	5/26/03	2 × 1800	2.7	5 × 3	25
	5/27/03	2 × 1800	2.9		
Pismis 24	5/20/01	4 × 900	4.2	2 × 3.5	23
		2 × 120			

Table 3. Measurements of equivalent widths of four Balmer lines.

Cluster	H_α	H_β	H_γ	H_δ
Windows	(6540–6586) Å	(4846–4884) Å	(4318–4364) Å	(4082–4124) Å
Markarian 38	6.5 ± 0.1	6.3 ± 0.1	6.70 ± 0.06	4.97 ± 0.09
NGC 6604	–2.2± 0.1	2.5 ± 0.1	1.3 ± 0.1	2.2 ± 0.1
Dolidze 34	3.6 ± 0.1	4.1 ± 0.1	4.3 ± 0.1	4.8 ± 0.1
Berkeley 80	7.6 ± 0.2	5.0 ± 0.2	9.0 ± 0.2	6.0 ± 0.3
ESO 429-SC2	4.8 ± 0.1	4.6 ± 0.1	4.1 ± 0.1	4.0 ± 0.1
ESO 445-SC74	4.85 ± 0.07	5.4 ± 0.1	4.3 ± 0.2	3.7 ± 0.2
Bochum 2	4.4 ± 0.1	5.1 ± 0.1	5.6 ± 0.1	2.4 ± 0.1
NGC 2311	9.6 ± 0.1	13.2 ± 0.1	8.0 ± 0.1	6.3 ± 0.1
NGC 2409	5.8 ± 0.1	4.4 ± 0.1	5.1 ± 0.1	4.2 ± 0.1
Ruprecht 2	6.3 ± 0.1	6.8 ± 0.1	4.9 ± 0.1	3.34 ± 0.07
Pismis 7	6.1 ± 0.1	7.7 ± 0.2	3.7 ± 0.2	2.7 ± 0.1
Hogg 9	9.70 ± 0.07	8.8 ± 0.1	8.62 ± 0.09	5.5 ± 0.1
Hogg 10	5.73 ± 0.08	5.51 ± 0.09	4.4 ± 0.1	4.29 ± 0.09
Basel 18	7.83 ± 0.7	8.5 ± 0.1	7.58 ± 0.09	5.18 ± 0.08
Trumpler 21	6.5 ± 0.1	6.22 ± 0.09	6.0 ± 0.1	5.1 ± 0.1
BH 151	1.7 ± 0.1	1.2 ± 0.2	4.6 ± 0.1	3.6 ± 0.1
NGC 5281	7.3 ± 0.1	6.9 ± 0.1	7.2 ± 0.1	6.5 ± 0.2
Lyngå 1	11.5 ± 0.1	11.5 ± 0.1	7.8 ± 0.2	2.0 ± 0.1
Pismis 20	2.5 ± 0.1	2.0 ± 0.1	2.0 ± 0.1	–0.2 ± 0.1
Hogg 22	4.2 ± 0.2	2.1 ± 0.1	2.9 ± 0.1	2.1 ± 0.1
NGC 6204	8.88 ± 0.07	7.3 ± 0.1	7.49 ± 0.08	6.38 ± 0.09
Pismis 24	4.2 ± 0.1	3.6 ± 0.1	3.5 ± 0.2	–0.2 ± 0.1

Table 4. Reddening and age determinations.

Cluster	$E(B-V)$	Age (Balmer) (Myr)	Age (template match) (Myr)	Adopted age (Myr)	Age (literature) (Myr)	References
Markarian 38	0.37 ± 0.03	~30	5–10	10 ± 10	9	1
NGC 6604	1.20 ± 0.05	<10	2–4	3 ± 1	4; 5	2; 3
Dolidze 34	0.70 ± 0.05	~700	500	600 ± 200	–	–
Berkeley 80	0.80 ± 0.05	500–1000	500	600 ± 200	300	4
ESO 429-SC2	0.30 ± 0.02	≤10	5–10	7.5 ± 2.5	–	–
ESO 445-SC74	0.00 ± 0.04	~5000	1000; 3000–4000	2500 ± 1500	–	–
Bochum 2	0.81 ± 0.02	10–50	2–4; 5–10	5 ± 3	5; 7	5; 6
NGC 2311	0.15 ± 0.03	200–500	200–350	300 ± 100	400	1
NGC 2409	0.25 ± 0.02	25–30	40; 45–75	50 ± 20	35	1
Ruprecht 2	0.10 ± 0.02	3000–4000	3000–4000	3500 ± 1000	–	–
Pismis 7	0.40 ± 0.03	2000–5000	3000–4000	3000 ± 1000	500	7
Hogg 9	0.05 ± 0.02	100–500	200–350	300 ± 100	–	–
Hogg 10	0.50 ± 0.04	10–30	20; 40	30 ± 10	36	8
Basel 18	0.30 ± 0.03	50–70	40; 45–75	50 ± 20	83	1
Trumpler 21	0.20 ± 0.03	30–50	20; 40	30 ± 10	25–30	9
BH 151	1.70 ± 0.05	<10	2–4	3 ± 1	–	–
NGC 5281	0.25 ± 0.04	10–50	20; 40	30 ± 10	45	10
Lyngå 1	0.38 ± 0.02	50–200	45–75	100 ± 50	100–125	11
Pismis 20	1.23 ± 0.05	<10	2–4	5 ± 1	5	12
Hogg 22	0.65 ± 0.03	<10	2–4; 5–10	4.5 ± 2.0	5	1
NGC 6204	0.40 ± 0.03	40–60	40	60 ± 10	80	13
Pismis 24	1.90 ± 0.05	<10	2–4; 5–10	5 ± 3	6	14

References: 1. Kharchenko et al. (2005); 2. Forbes & Dupuy (1978); 3. Barbon et al. (2000); 4. Carraro et al. (2005); 5. Turbide & Moffat (1993); 6. Munari & Carraro (1995); 7. Ahumada (2005); 8. Clariá (1976); 9. Giorgi et al. (2001); 10. Sanner et al. (2001); 11. Vázquez et al. (2003); 12. Vázquez et al. (1995), 13. Carraro & Munari (2004); 14. Massey et al. (2001).

Appendix A: Discussion of individual clusters

In Ahumada et al. (2000, 2001) we presented the results corresponding to a sample of 20 small angular diameter Galactic open clusters observed at CASLEO before the year 2002. The determination of the fundamental cluster parameters was carried out by using the template cluster spectral libraries available until 2002, namely, Bica (1988), Bica et al. (1990) and Santos et al. (1995). The results obtained for this cluster sample, together with many integrated spectra from the existing literature, were the basis to develop Piatti et al.'s (2002) new library of solar-metallicity open-cluster templates. This library, which is used in the present study, is probably the most complete open cluster template spectral library available.

The present cluster sample complements those of Ahumada et al. (2000, 2001). As far as we are aware, there are no data for six open clusters of the present sample. They are: Dolidze 34, ESO 429-SC2, ESO 445-SC74, Ruprecht 2, BH 151 and Hogg 9. Therefore, the foreground reddening values and ages derived here are the first of their kind. We briefly discuss the results obtained for each of the 22 open clusters.

A.1. Markarian 38

This object, also known as Biurakan 5 (Iskurzdajan 1959), was first catalogued as an open cluster by Markarian (1951). This is a small and compact cluster classified as Trumpler class I1p by AH03. Markarian 38 is located at less than 12° from the Galactic centre direction. The cluster integrated spectrum, without the contribution of the comparatively bright blue star HD 167287 and corrected for $E(B-V) = 0.37$, matches very closely that of the Yb1 template of 5–10 Myr (Fig. A.1). Both the reddening value and the age of the template are consistent with the $E(B-V)$ colour excess (=0.34) and with the earliest photometric spectral type (B1) estimated by Vogt & Moffat (1975) from a preliminary photometric *UBV* study. Based on *RGU* photometry of poorer quality, Grubissich & Becker (1980) obtained $E(G-R) = 0.55$, equivalent to $E(B-V) = 0.40$ (Steilin 1968). More recently, Kharchenko et al. (2005) applied homogeneous methods and algorithms to determine astrophysical parameters for 520 Galactic open clusters. For Markarian 38 they report $E(B-V) = 0.30$, $d = 1545$ pc and an age of 9 Myr, in good agreement with our results. Figure A.2 shows the comparison between the individual spectrum of HD 167287, corrected for $E(B-V) = 0.37$, and the B3/5 I template from Silva & Cornell (1992, hereafter SC92). Undoubtedly, this is a B-type supergiant cluster member. HD 167287 was also classified as B1 Iab by Houck & Cowley (1975), in good agreement with the present classification.

A.2. NGC 6604

NGC 6604 is a compact cluster which belongs to the Trumpler class I3mn (AH03). It is located at less than 19° from the Galactic centre direction. Also known as Cr 373 (Collinder 1931) or Markarian 39 (Markarian 1951), NGC 6604 is associated with the HII region RCW 167 (Rodgers et al. 1960). This cluster includes several luminous OB stars (Stephenson & Sanduleak 1971), which indicates that it is extremely young. Although the light of the cluster is probably dominated by that of the bright star HD 167971 – an O8f supergiant star according to Forbes & Dupuy (1978) – the cluster integrated spectrum, corrected for $E(B-V) = 1.20$, compares reasonably well with the Ya1 template of 2–4 Myr (Fig. A.3). The weakness of

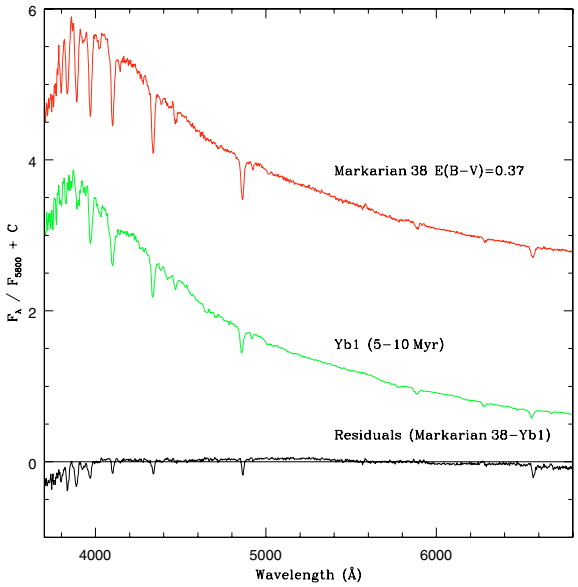

Fig. A.1. Integrated spectrum of Markarian 38 corrected for the derived $E(B-V)$ colour excess (*top*), the template spectrum which best matches it (*middle*), and the flux residuals according to $(F_{\rm cluster} - F_{\rm template})/F_{\rm cluster}$ (*bottom*). Units as in Fig. 1.

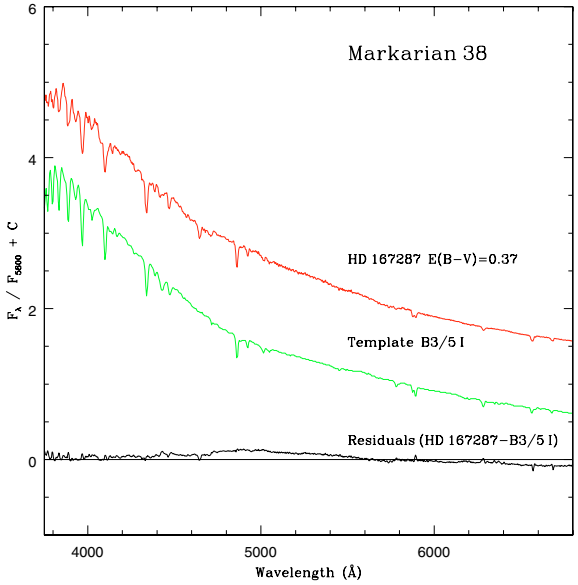

Fig. A.2. Individual spectrum of the bright star HD 167287 of Markarian 38 corrected for the derived $E(B-V)$ colour excess (*top*), the SC92 template spectrum which best matches it (*middle*), and the flux residuals according to $(F_{\rm cluster} - F_{\rm template})/F_{\rm cluster}$ (*bottom*). Units as in Fig. 1.

Balmer absorption lines in the cluster spectrum also indicates $t < 10$ Myr. An alternative comparison with the Ya1_WR template, using the same reddening, is presented in Fig. A.3. As explained by Piatti et al. (2002), the Ya1_WR template takes into account the possible presence of dominant luminous stars (supergiant and Wolf-Rayet (WR) stars). The emission lines observed in the cluster spectrum are very likely to be due to the O8f star.

Moffat & Vogt (1975c) obtained *UBV* photoelectric photometry of 11 comparatively bright stars in the cluster field. They showed the interstellar reddening in front of this cluster to be variable, the mean value being $\langle E(B-V)\rangle = 1.01$, provided

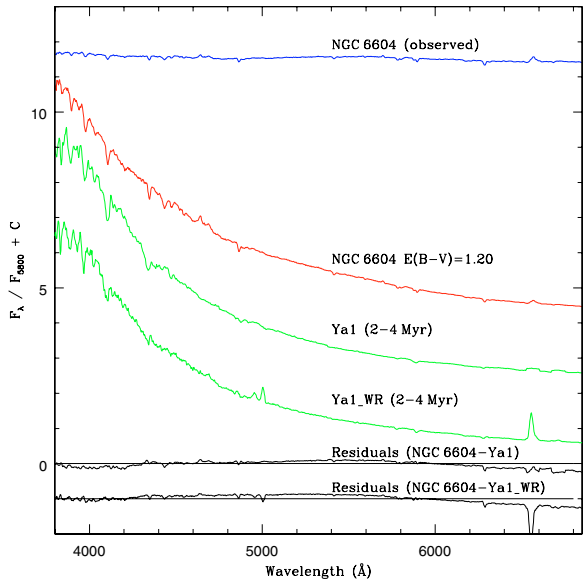

Fig. A.3. *From top to bottom*: observed integrated spectrum of NGC 6604, the cluster spectrum corrected for the derived $E(B-V)$ colour excess, the Ya1 and Ya1_WR template spectra of (2−4) Myr, and the flux residuals according to $(F_{\rm cluster} - F_{\rm template})/F_{\rm cluster}$. Units as in Fig. 1.

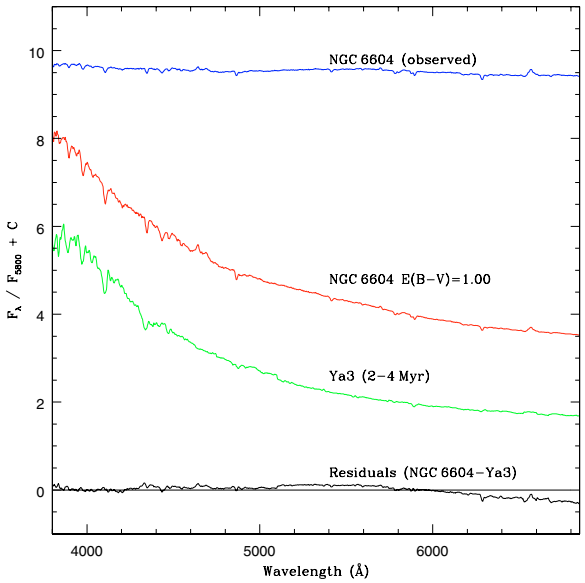

Fig. A.4. *From top to bottom*: observed integrated spectrum of NGC 6604, the cluster spectrum corrected for $E(B-V) = 1.00$, the Ya3 template spectrum of (2−4) Myr, and the flux residuals according to $(F_{\rm cluster} - F_{\rm template})/F_{\rm cluster}$. Units as in Fig. 1.

that the two stars with the largest reddenings are not considered. On the other hand, Forbes & Dupuy (1978) estimated an age of ∼4 Myr and a mean colour excess $\langle E(B-V)\rangle = 0.96$, based on photoelectric and photographic *UBV* data. They also confirmed that the central star HD 167971 is an O8f supergiant cluster member. More recently, Barbon et al. (2000) obtained almost the same cluster parameters using *CCD BVI* photometry and echelle spectroscopy. These ages show very good agreement with the age obtained here by the template matching method (Table 4). However, the spectroscopic reddening clearly turns out to be larger than the photometric one. It could be possible that NGC 6604, due to its youth, includes a large amount of associated internal dust; this might be a possible cause of the mentioned discrepancy. If this were the case, a comparison with the Ya3 template of (2−4) Myr could clarify the problem. For this reason, we compare in Fig. A.4 the cluster spectrum with that template. Note that if the observed cluster spectrum is corrected for $E(B-V) = 1.0$, the comparison with the Ya3 template is excellent. Since previous studies on this object clearly show that the mean $E(B-V)$ colour excess of NGC 6604 is about 1.0, we conclude that it is definitely a very young cluster with an internal reddening of about 0.20 mag. It is important to define templates corresponding to very young clusters which have a significant amount of internal dust. Unfortunately, it was not possible to obtain an individual extraction of the bright star HD 167971 without including neighbouring stars.

A.3. Dolidze 34

This object was first catalogued as an open cluster by Dolidze (1961) and, as far as we are aware, there is no previous data about it. Dolidze 34 barely stands out as a small handful of comparatively bright stars without central concentration. It looks like other stellar clusters which have been proven to be open cluster remnants. A clear example is Ruprecht 3, which is quite similar to Dolidze 34. According to Pavani et al. (2003), Ruprecht 3 is very likely an intermediate-age open cluster remnant. Although

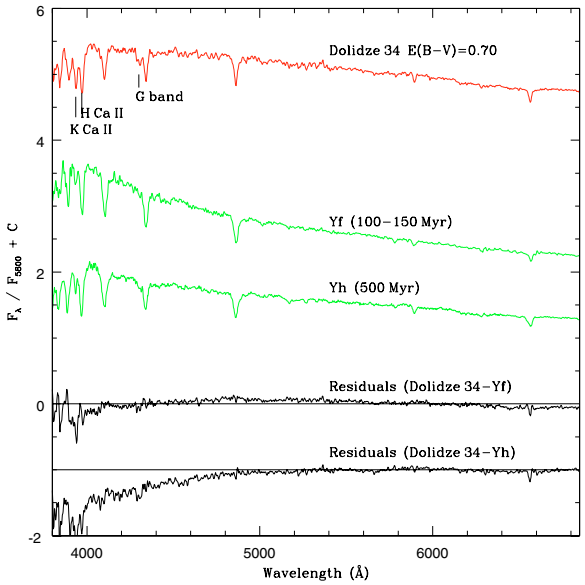

Fig. A.5. Integrated spectrum of Dolidze 34 corrected for the derived $E(B-V)$ value (*top*), the Yf (100−150 Myr) and Yh (500 Myr) template spectra (*middle*), and the flux residuals according to $(F_{\rm cluster} - F_{\rm template})/F_{\rm cluster}$ (*bottom*). Units as in Fig. 1.

the physical reality of Dolidze 34 has not yet been confirmed, the four brightest stars in the cluster field could be physically related. To explore this possibility, we compare in Fig. A.5 the integrated cluster spectrum – basically that of the four brightest stars – corrected for $E(B-V) = 0.70$, with the Yf and Yh templates of (100−150) Myr and 500 Myr, respectively. The continuum distribution, the presence of the G-band (∼4300 Å) and the intensity of the H and K CaII lines in the observed spectrum favour the choice of the template Yh. In addition, G-band intensity indicates that Dolidze 34 could be even older than the template Yh. As Balmer lines suggest an age of ∼700 Myr, we adopted 600 ± 200 Myr for the cluster (Table 4). In Fig. A.6 the observed individual spectrum of HD 172747, the brightest star

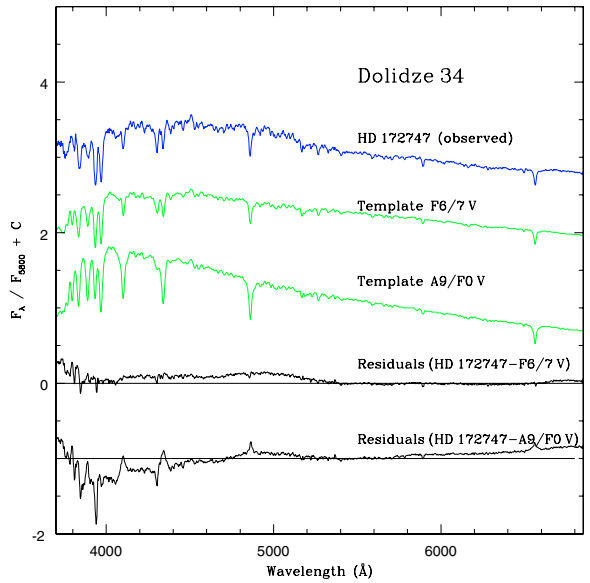

Fig. A.6. Observed individual spectrum of the bright star HD 172747 of Dolidze 34 (*top*), the SC92 F6/5 V and A9/F0 V template spectra (*middle*), and the flux residuals according to $(F_{\rm cluster} - F_{\rm template})/F_{\rm cluster}$ (*bottom*). Units as in Fig. 1.

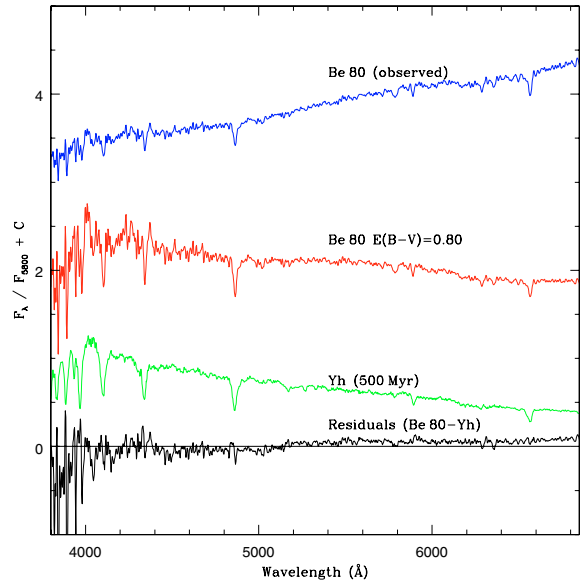

Fig. A.7. *From top to bottom*: the observed integrated spectrum of Berkeley 80, the cluster spectrum corrected for the derived $E(B-V)$ value, the template spectrum which best matches it, and the flux residuals according to $(F_{\rm cluster} - F_{\rm template})/F_{\rm cluster}$. Units as in Fig. 1.

of Dolidze 34, compares well with both the F6/7 V and A9/F0 V templates from the SC92 spectral library. The F6/7 V template better matches the cluster spectrum for $\lambda > 5300$ Å. For $\lambda < 5300$ Å, the best fit corresponds to a spectral type in between the two SC92 templates, i.e., ∼F3/4 V. Regardless of Dolidze 34 being a cluster or a remnant, HD 172747 is a foreground star not physically associated with the cluster itself.

A.4. Berkeley 80

Being a rich, moderately concentrated, open cluster, it is surprising that AH03 classified it as II1p type. Berkeley 80 lies in a high

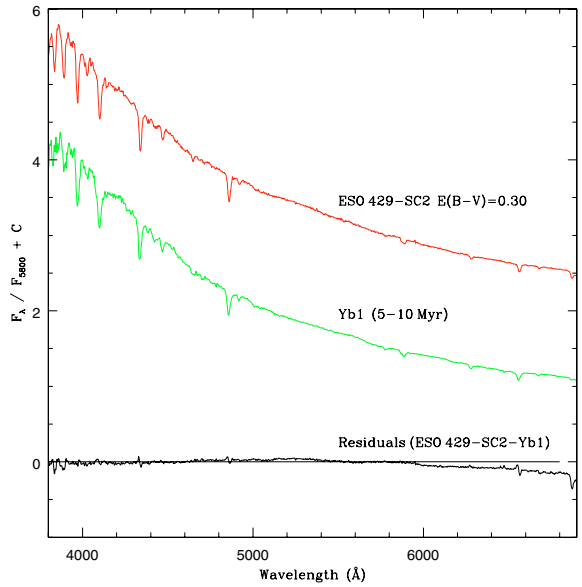

Fig. A.8. Integrated spectrum of ESO 429-SC2 corrected for the derived $E(B-V)$ value (*top*), the template spectrum which best matches it (*middle*),and the flux residuals according to $(F_{\rm cluster} - F_{\rm template})/F_{\rm cluster}$ (*bottom*). Units as in Fig. 1.

density stellar region and is barely visible in the blue DSS image. Despite the rather low S/N ratio, the integrated spectrum of Berkeley 80 shows typical features of a Hyades-like age open cluster. We determined simultaneously its age and reddening by using the Yh template of 500 Myr (Fig. A.7). Since the Balmer lines indicate a somewhat older age than that of the template, we tentatively adopted $E(B-V) = 0.80 \pm 0.05$ and $t = 600 \pm 200$ Myr for this cluster (Table 4). Based on *CCD BVI* photometry, Carraro et al. (2005) have recently derived a somewhat larger reddening, $E(B-V) = 1.1$, and an age of ∼300 Myr from theoretical isochrone fitting.

A.5. ESO 429-SC2

This cluster was catalogued by Lauberts (1982). Like Dolidze 34, it has not yet been studied. The observed integrated spectrum of ESO 429-SC2 shows an excellent resemblance to the Yb1 template of (5−10) Myr, provided that it has been previously corrected for $E(B-V) = 0.30$ (Fig. A.8). The continuum distribution, the Balmer jump and also the presence and depth of the spectral lines are nearly identical in both spectra. The EWs of the Balmer lines also indicate $t \leq 10$ Myr.

A.6. ESO 445-SC74

As for most of the clusters recognised in Lauberts (1982), ESO 445-SC74 has not been the object of previous studies. AH03 refer to this cluster as belonging to Trumpler class II3. Figure A.9 shows a comparison of the observed integrated cluster spectrum with both the Ia (1 Gyr) and Ib (3−4 Gyr) template spectra. In general terms, the observed spectrum looks like template Ia, particularly in the presence and intensity of the spectral lines for wavelengths longer than 4600 Å. However, both spectral lines and molecular bands better resemble those of the oldest template for shorter wavelengths. Note in the integrated spectrum of ESO 445-SC74, the presence of CN bands in the region of 4200 Å, which are typical of old objects. Since the Balmer

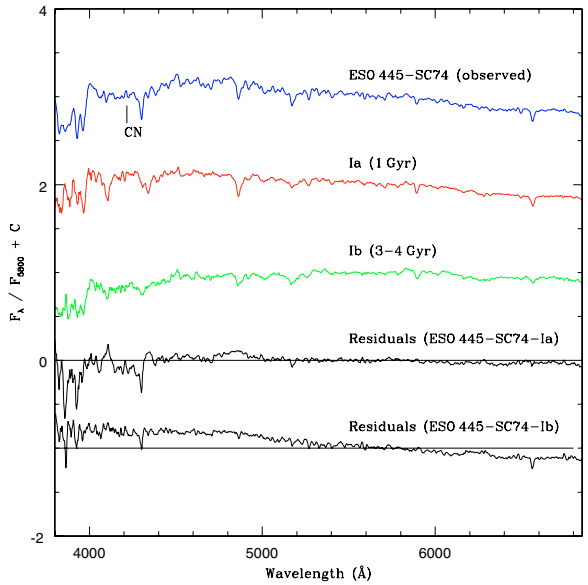

Fig. A.9. *From top to bottom*: the observed integrated spectrum of ESO 445-SC74, the Ia (1 Gyr) and Ib (3−4 Gyr) template spectra, and the flux residuals according to $(F_{\rm cluster} - F_{\rm template})/F_{\rm cluster}$. Units as in Fig. 1.

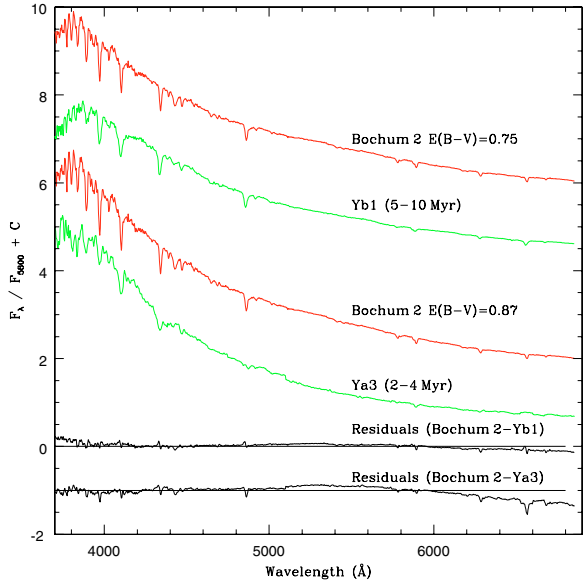

Fig. A.10. *From top to bottom*: the integrated spectrum of Bochum 2 corrected for $E(B-V) = 0.75$, the Yb1 template of (5−10) Myr, the cluster spectrum corrected for $E(B-V) = 0.87$, the Ya3 template of (2.4) Myr, and the corresponding flux residuals between both comparisons. Units as in Fig. 1.

age is ∼5 Gyr, we adopted for ESO 445-SC74, an average of the two considered template ages, i.e., 2.5 Gyr. It should be noted that the cluster spectral features could suffer stochastic effects as this is a relatively poor star cluster.

A.7. Bochum 2

This is a very compact and elongated object in Monoceros classified as I1p by AH03. Moffat & Vogt (1975a) measured 8 stars photoelectrically in the *UBV* system and derived $E(B-V) = 0.89 \pm 0.04$. The particular distribution of the cluster stars in the sky allowed us to make different individual spectral extractions,

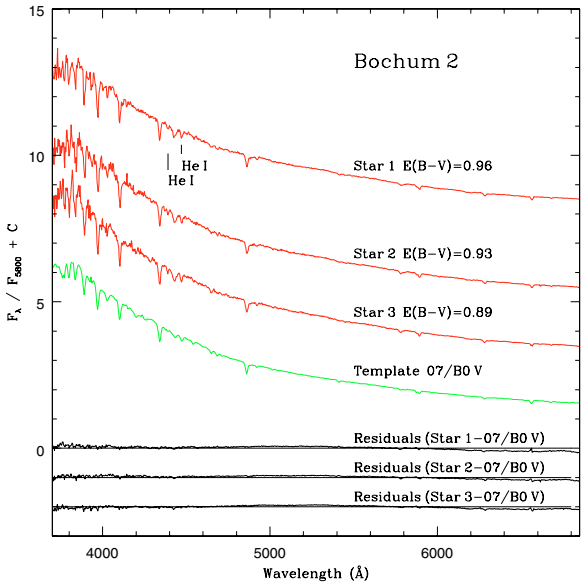

Fig. A.11. *From top to bottom*: the individual reddening-corrected spectra of stars 1, 2 and 3 (MV73) of Bochum 2, the SC92 template spectrum which best matches it (*middle*), and the flux residuals according to $(F_{\rm cluster} - F_{\rm template})/F_{\rm cluster}$. Units as in Fig. 1.

thus avoiding contamination from field stars. Figure A.10 shows the cluster spectrum corrected for $E(B-V) = 0.75$ compared to the Yb1 template (5−10) Myr. The similarity between these two spectra is evident. An alternative match is shown in the same figure, where we compare the spectrum of Bochum 2, corrected for $E(B-V) = 0.87$, with the younger Ya3 template of (2−4) Myr. In the first case, there is a more evident similarity between the Balmer lines than in the second case. However, the opposite case results when only the continuum distribution for $\lambda < 5000$ Å is considered. For Bochum 2 we adopted reddening and age values between those of these two templates (Table 4). Figure A.11 presents the individual observed spectra of the bright stars 1 ($V = 11.31$), 2 ($V = 10.86$) and 3 ($V = 11.15$) photoelectrically observed by Moffat & Vogt (1975a). This figure shows the reddening-corrected spectra of these stars and the O7/B0 V template from SC92. Disregarding a few slight differences, the spectral features of these three stars are in good agreement with those of the selected template. Since their reddening values are very similar, we can conclude that they are very likely to be early-type cluster members. The SC92 O7/B0 V template was chosen because of the presence of the HeI 4471 Å and HeI 4390 Å lines, which are different from those in the earlier O5 template. The spectral classification we made and the foreground reddening values derived here should be only considered as estimates, since the spectral resolution of SC92's library is quite limited. The reddening and age values derived here for Bochum 2 show excellent agreement with the values determined by Munari & Carraro (1995) from a spectrophotometric study.

A.8. NGC 2311

NGC 2311 or Cr 123 (Collinder 1931) is a moderately concentrated group of stars as seen in the blue DSS image. Even though the S/N ratio is rather low, the integrated cluster spectrum, corrected for $E(B-V) = 0.15$, compares well with that of the Yg template of 200−350 Myr (Fig. A.12). The age of the template is close to that inferred from the EWs of the Balmer lines (Table 4). Therefore, NGC 2311 is a scarcely reddened

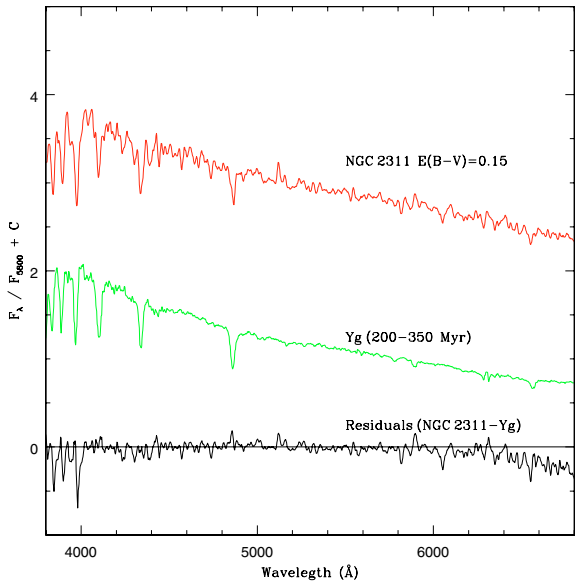

Fig. A.12. Integrated spectrum of NGC 2311 corrected for the derived $E(B-V)$ value (*top*), the template spectrum which best matches it (*middle*), and the flux residuals according to $(F_{\rm cluster} - F_{\rm template})/F_{\rm cluster}$ (*bottom*). Units as in Fig. 1.

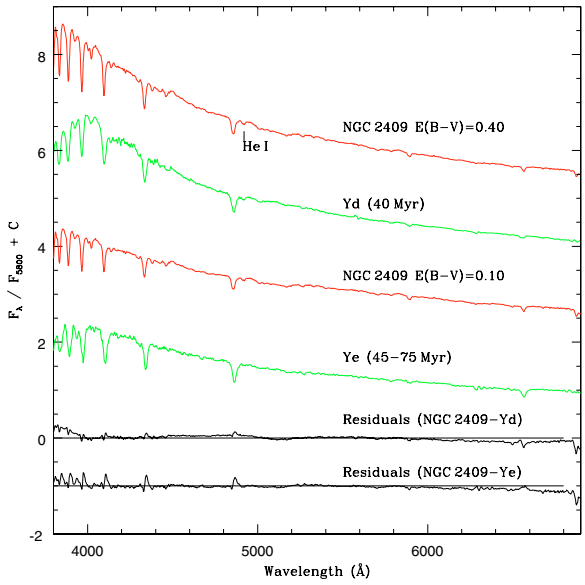

Fig. A.13. *From top to bottom*: the integrated spectrum of NGC 2409 corrected for $E(B-V) = 0.40$, the Yd template spectrum of 40 Myr, the cluster spectrum corrected for $E(B-V) = 0.10$, the Ye template spectrum of 60 Myr, and the corresponding flux residuals between both comparisons. Units as in Fig. 1.

moderately young cluster. The values adopted are compatible with those recently reported by Kharchenko et al. (2005).

A.9. NGC 2409

This object, equivalent to Bochum 4 according to AH03, is formed by several stars surrounding the bright star BD -16°1994, whose equatorial coordinates are: $\alpha_{2000} = 7^{\rm h}31^{\rm m}37^{\rm s}$, $\delta_{2000} = -17°11.7'$. NGC 2409 should not be mistaken for Bochum 5, an elongated open cluster located north-east of Bochum 4, centred at $\alpha_{2000} = 7^{\rm h}32.1'$, $\delta_{2000} = -16°57.3'$. The observed integrated spectrum of NGC 2409 resembles the Yd template of 40 Myr (Fig. A.13), as long as it has been previously corrected for $E(B-V) = 0.40$. The age of this template is in good agreement with that obtained from the Balmer lines (25−30 Myr). Nevertheless, as shown in Fig. A.13, a reasonable match is also found when the cluster spectrum is compared to the Ye template of (45−75) Myr, once it has been corrected for a significantly smaller reddening. When the cluster spectrum is compared with the Yd template, an excellent agreement in the continuum distribution for $\lambda > 4000$ Å is seen. The main lines in this spectral region clearly appear both in NGC 2409 and in the Yd template, particularly the HeI 4921 Å line. The comparison in the region of the 4000 Å break is, however, not good. On the other hand, when the cluster spectrum is compared with the Ye template, a better comparison towards $\lambda < 4000$ Å and a poorer match for $\lambda > 4000$ Å is observed. We adopted intermediate reddening and age values for NGC 2409, i.e., 50 ± 20 Myr and $E(B-V) = 0.25 \pm 0.02$. Both values are slightly larger than those reported by Kharchenko et al. (2005).

A.10. Ruprecht 2

This is a loose group of stars in Canis Major with no central concentration. Its integrated spectrum shows typical features of intermediate-age clusters (Fig. 1) and looks like that of Ruprecht 3, a remnant of an intermediate-age open cluster

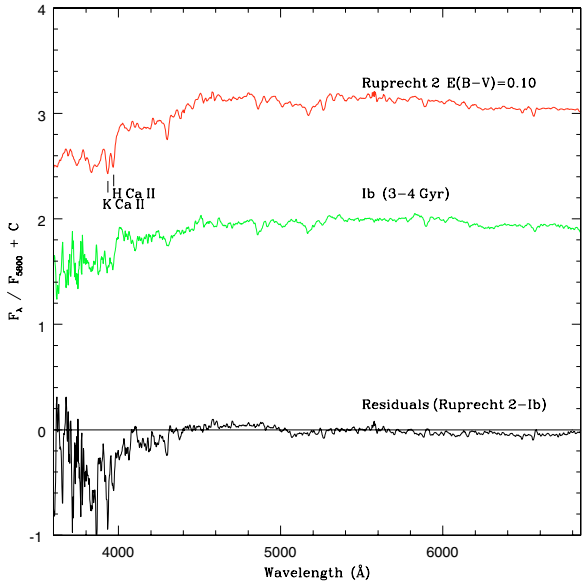

Fig. A.14. Integrated spectrum of Ruprecht 2 corrected for the derived $E(B-V)$ value (*top*), the template spectrum which best matches it (*middle*), and the flux residuals according to $(F_{\rm cluster} - F_{\rm template})/F_{\rm cluster}$ (*bottom*). Units as in Fig. 1.

(Pavani et al. 2003). The solution by template match for Ruprecht 2 yields an age of ∼3.5 Gyr and $E(B-V) = 0.10$ (Fig. A.14). This age is in very good agreement with that derived from the EWs of the Balmer lines (3−4 Gyr). Note the similarity between the H and K CaII lines, the continuum distribution and the depth of the lines of the spectrum of Ruprecht 2 and the same features of the selected template. In Fig. A.15 we present the reddening-corrected individual spectrum of the comparatively bright star CD -29°3349 and the G0/4 III template from SC92. The acceptable coincidence between the colour excess derived for CD -29°3349 and that of the G0/4 III template suggests that this star is very likely to be a cluster red giant.

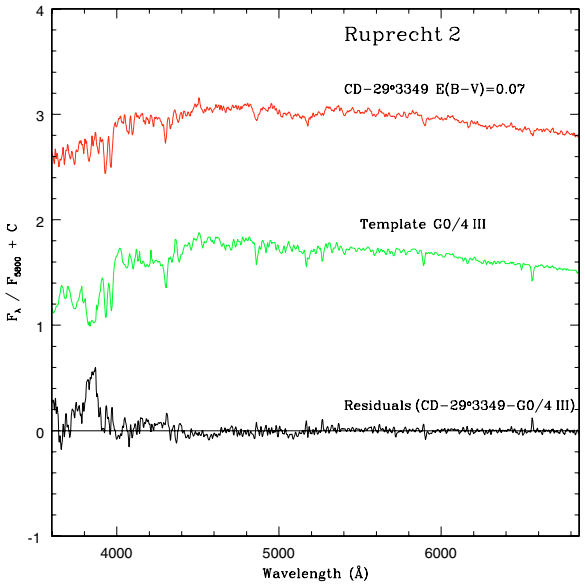

Fig. A.15. Individual spectrum of one of the dominant stars of Ruprecht 2 (CD-29°3349) corrected for reddening (*top*), the SC92 template spectrum which best matches it (*middle*), and the flux residuals according to $(F_{\rm cluster} - F_{\rm template})/F_{\rm cluster}$ (*bottom*). Units as in Fig. 1.

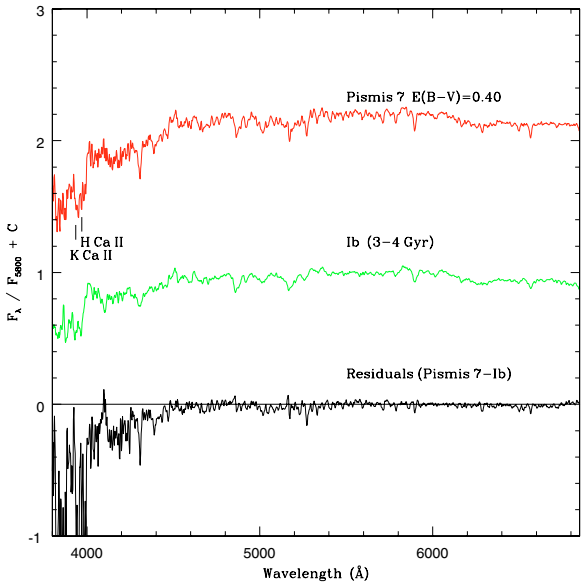

Fig. A.16. Integrated spectrum of Pismis 7 corrected for the derived $E(B-V)$ value (*top*), the template spectrum which best matches it (*middle*), and the flux residuals according to $(F_{\rm cluster} - F_{\rm template})/F_{\rm cluster}$ (*bottom*). Units as in Fig. 1.

A.11. Pismis 7

This small group of stars, also known as BH 43 (van den Bergh & Hagen 1975), was first recognised as an open cluster by Pismis (1959). Its low surface brightness explains the comparatively low S/N ratio of the integrated spectrum. However, H and K CaII lines as well as many other spectral lines typical of intermediate-age clusters are seen in such spectra. The best match is found for the Ib template of (3−4) Gyr, using $E(B-V) = 0.40$, in very good agreement with the Balmer age (Fig. A.16, Table 4). The results obtained here are not in agreement with those of Ahumada (2005), which are based on *CCD BVRI* poor quality photometry. The cluster spectrum could suffer from stochastic effects, as in Ruprecht 3 for example (Pavani et al. 2003).

A.12. Hogg 9

Hogg 9, a small group of ∼10 stars in Carina, was first recognised as a probable cluster by Hogg (1965a,b). Nonetheless, based on *UBV* photoelectric photometry of 9 bright stars in the cluster field, Moffat & Vogt (1975b) considered this sparse group of stars as a probable random fluctuation of the field stellar density rather than a physical system. If indeed Hogg 9 is an open cluster, then it is a slightly reddened, moderately young object since the comparison between its integrated spectrum, corrected for $E(B-V) = 0.05$, and the Yg template of (200−350) Myr is excellent (Fig. A.17). According to the Balmer lines, Hogg 9 should be ∼300 Myr old, in good agreement with the template match. Radial velocity measurements of a few stars in the cluster field could help to confirm or reject the physical reality of Hogg 9.

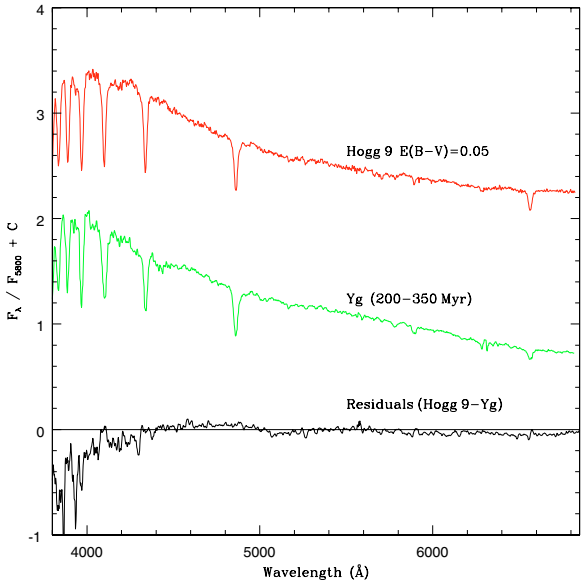

Fig. A.17. Integrated spectrum of Hogg 9 corrected for the derived $E(B-V)$ value (*top*), the template spectrum which best matches it (*middle*), and the flux residuals according to $(F_{\rm cluster} - F_{\rm template})/F_{\rm cluster}$ (*bottom*). Units as in Fig. 1.

A.13. Hogg 10

Like Hogg 9, this is a small and concentrated group of stars in Carina located south of NGC 3572. Classified as a I3p-type system by AH03, Hogg 10 was first recognised as an open cluster by Hogg (1965a,b). The cluster's light is dominated by that of the bright star HD 97253, an O5.5III(f) star according to Walborn (1973). The cluster spectrum (without the contribution of HD 97253), compares well with the 20 Myr template, using $E(B-V) = 0.50$ (Fig. A.18). Yet, since the Balmer lines resemble more closely those of the 40 Myr template (Fig. A.18), we adopted for Hogg 10, an intermediate value of 30 Myr. These results are compatible with those obtained from *UBV*-H_β photometry by Clariá (1976), who derived $E(B-V) = 0.49$ and an age of 36 Myr. As shown in Fig. A.19, the individual spectrum of HD 97253, corrected for $E(B-V) = 0.51$, is very similar to that of an O7/B1 III star from SC92. This fact confirms that HD 97253 is very likely to be a cluster blue giant. Note,

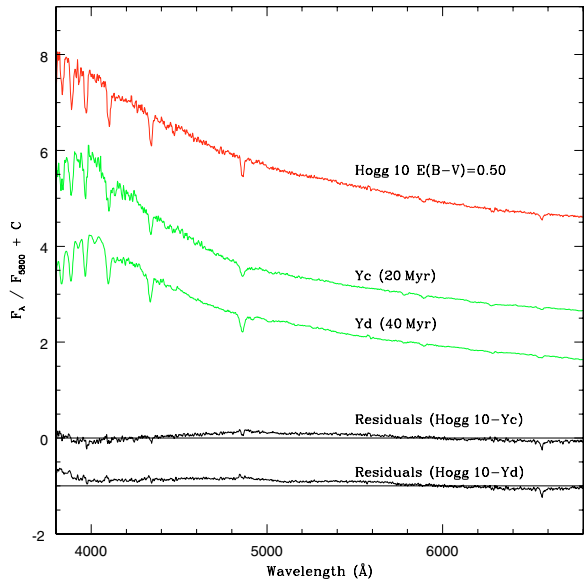

Fig. A.18. Integrated spectrum of Hogg 10 corrected for the derived $E(B-V)$ value (*top*), the Yc (20 Myr) and Yd (40 Myr) template spectra (*middle*), and the corresponding residuals between both comparisons (*bottom*). Units as in Fig. 1.

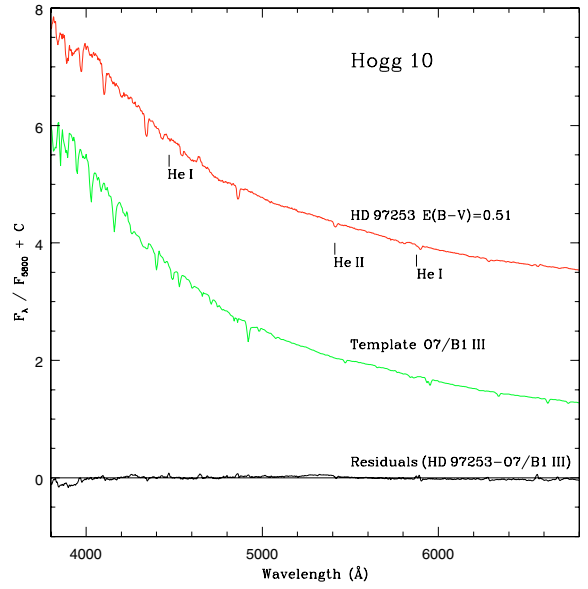

Fig. A.19. Individual spectrum of the dominant star HD 97253 of Hogg 10 corrected for reddening (*top*), the SC92 template spectrum which best matches it (*middle*), and the flux residuals according to $(F_{\rm cluster} - F_{\rm template})/F_{\rm cluster}$ (*bottom*). Units as in Fig. 1.

however, that HeI 4471 Å and HeI 5876 Å lines appear to be slightly fainter in the template than in the star, while HeII 5412 Å is scarcely visible in the template. These features indicate that HD 97253 should be somewhat earlier than the O7/B1 III template, in good agreement with Walborn's (1973) spectral classification. Given the good S/N ratio of the integrated spectrum of Hogg 10, it could be averaged with other spectra of the same quality and similar charecteristics to define a new open cluster template of 30 Myr to be added to the Piatti et al. (2002) spectral library (Sect. 5.2).

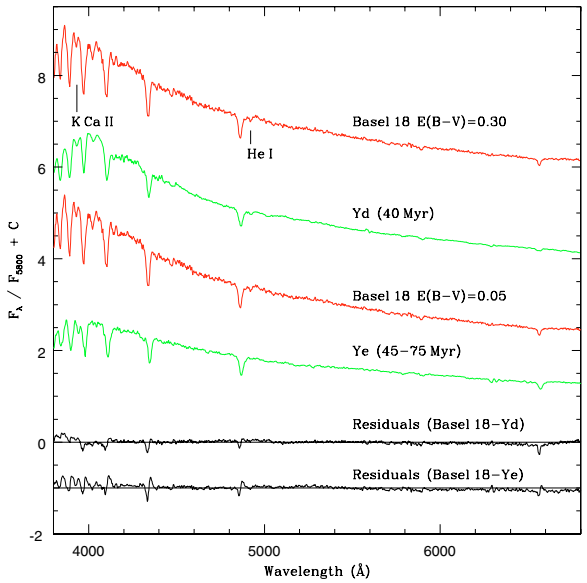

Fig. A.20. *From top to bottom*: the integrated spectrum of Basel 18 corrected for $E(B-V) = 0.30$, the Yd template spectrum of 40 Myr, the cluster spectrum corrected for $E(B-V) = 0.05$, the Ye template spectrum of (45−75) Myr, and the corresponding flux residuals between both comparisons. Units as in Fig. 1.

A.14. Basel 18

Basel 18, first reported by Fenkart et al. (1977), is a sparse group of stars in Centaurus dominated by the bright star HD 116841. The spectral features of Basel 18 match quite well those of NGC 2409. In fact, the integrated spectrum of Basel 18, corrected for $E(B-V) = 0.30$, exhibits good agreement with the Yd template of 40 Myr, while the spectrum corrected for $E(B-V) = 0.05$, compares reasonably well with the Ye template of (45−75) Myr (Fig. A.20). In the first comparison, HeI 4921 Å and K CaII lines are clearly visible both in the cluster spectrum and in the template. This is not the case in the second comparison. When we consider in the second case both the depth of the Balmer lines and the blue continuum distribution, a better agreement is achieved. Since the Balmer lines indicate an age between 40 and 70 Myr (Table 4), we adopted for Basel 18 intermediate values of 50 ± 20 Myr and $E(B-V) = 0.30 \pm 0.03$. Kharchenko et al. (2005) recently reported a larger reddening value, $E(B-V) = 0.51$, and an age of 83 Myr. As shown in Fig. A.21, the individual spectrum of the bright star HD 116841, corrected for $E(B-V) = 0.33$, is very similar to that of a K4 III type star from SC92. Consequently, HD 116841 is very likely to be a cluster red giant.

A.15. Trumpler 21

This is a conspicuous group of stars classified both by Ruprecht (1966) and by AH03 as I2p type. Also known as BH 148 (van den Bergh & Hagen 1975) or Cr 274 (Collinder 1931), Trumpler 21 was first recognised as an open cluster in Centaurus by Trumpler (1930). The EWs of the Balmer lines as much as the best template match – using $E(B-V) = 0.20$ – yield an age of about 40 Myr (Fig. A.22). Considering that the 4000 Å break in the cluster spectrum better resembles that of the Yc template of 20 Myr (Fig. A.22), we adopted for the cluster an age of 30 ± 10 Myr. The age and $E(B-V)$ colour excess determined here are in good agreement with the values derived photometrically

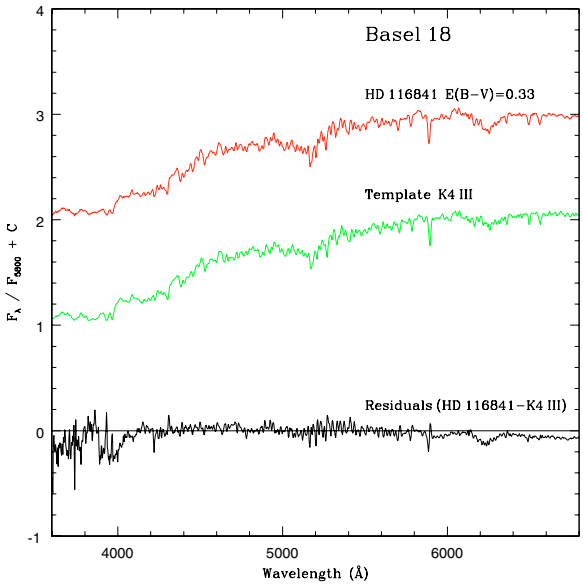

Fig. A.21. Individual spectrum of the dominant star HD 116841 of Basel 18 corrected for reddening (*top*), the SC92 template spectrum which best matches it (*middle*), and the flux residuals according to $(F_{\rm cluster} - F_{\rm template})/F_{\rm cluster}$ (*bottom*). Units as in Fig. 1.

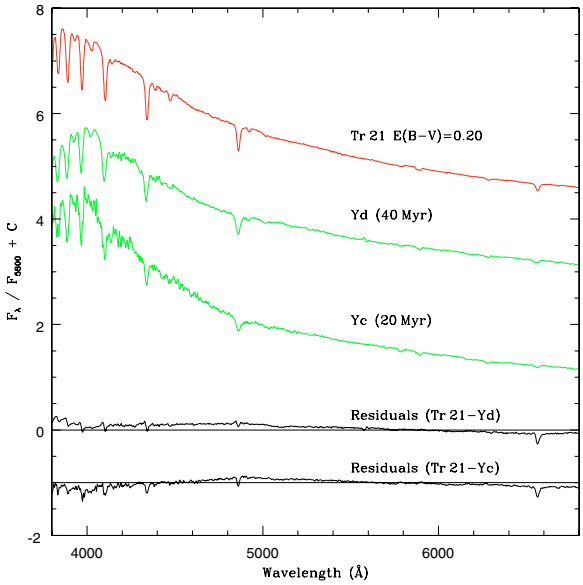

Fig. A.22. Integrated spectrum of Trumpler 21 corrected for the derived $E(B-V)$ value (*top*), the Yd (40 Myr) and Yc (20 Myr) template spectra (*middle*), and the corresponding flux residuals between both comparisons (*bottom*). Units as in Fig. 1.

by MV73, Peterson & Fitzgerald (1988) and Giorgi et al. (2001). The integrated spectrum of Trumpler 21 was averaged with other spectra of similar quality in order to define a new open cluster template of 30 Myr (Sect. 5.2).

A.16. BH 151

As far as we know, no previous data exist for this object first reported as an open cluster in Centaurus by van den Bergh & Hagen (1975). BH 151, classified as I2mn by AH03, is embedded in the small nebula RCW 79 (Dutra et al. 2003; Rodgers et al. 1960). As shown in Fig. 1, the S/N ratio of the observed

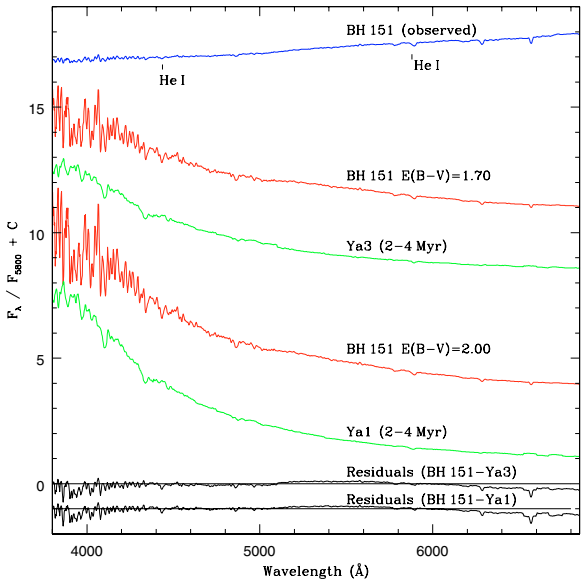

Fig. A.23. *From top to bottom*: the observed integrated spectrum of BH 151, the cluster spectrum corrected for $E(B-V) = 1.70$, the Ya3 template spectrum of (2−4) Myr, the cluster spectrum corrected for $E(B-V) = 2.00$, the Ya1 template spectrum of (2−4) Myr, and the corresponding flux residuals between both comparisons. Units as in Fig. 1.

spectrum of BH 151 is low for $\lambda < 4500$ Å. Nevertheless, to determine the cluster parameters, we compared the cluster spectrum with two different templates of (2−4) Myr, so as to consider the possible existence of internal dust in this very young cluster. In Fig. A.23, we compare the observed spectrum – corrected for different reddening values – with the templates Ya3 and Ya1 of (2−4) Myr. Although both comparisons appear acceptable, the $E(B-V)$ value derived in the comparison with Ya1 indicates that the internal reddening in BH 151 is ∼0.30 mag. The total reddening of BH 151 is $E(B-V) = 1.70$. The Balmer lines suggest an age younger than 10 Myr; it is well known, however, that these lines are not a good age indicator for very young clusters (Bica & Alloin 1986a). The presence of the HeI 4437 Å and HeI 5876 Å lines, which are good age indicators, reinforces the age determined from the template match.

A.17. NGC 5281

This comparatively bright open cluster is also known as BH 152 (van den Bergh & Hagen 1975), Mel 120 (Melotte 1915) or Cr 276 (Collinder 1931). Classified as I3m by AH03, the cluster's light is dominated by four bright stars (up to $V = 6.6$ mag) located almost along the same line on the sky as seen in the blue DSS image. Photoelectric *UBV* photometry of 18 stars by MV73 yields $E(B-V) = 0.26$ and a distance of 1.3 kpc, the earliest photometric spectral type being B5. The brightest star in the cluster field (HD 119699, No. 1 from MV73, $V = 6.61$), classified as A2 II by Stephenson & Sanduleak (1971), is a Ib-type supergiant according to MV73. Its position in the *UBV* diagrams is compatible with cluster membership. Another bright star in the field is CPD -62°3559 (No. 11 from MV73, $V = 8.39$), a K4 Ib-II star reddened by $E(B-V) = 0.23$ (Clariá et al. 1989). In a more recent photometric and kinematic study, Sanner et al. (2001) estimated the age of NGC 5281 in 45 ± 10 Myr by fitting theoretical isochrones. They derived $E(B-V) = 0.20 \pm 0.02$, which is somewhat smaller than that of MV73.

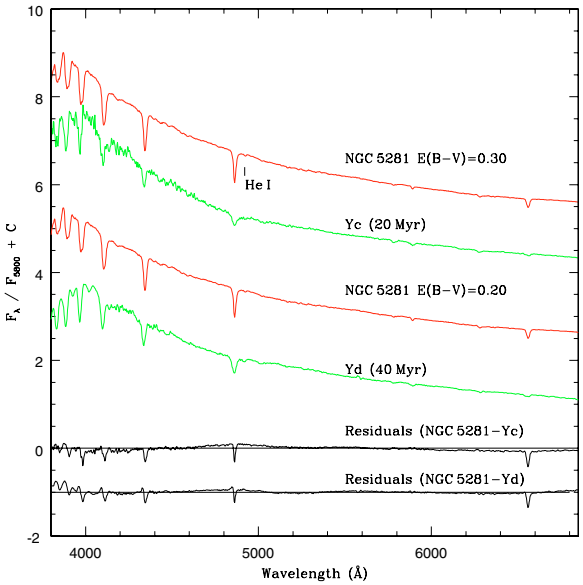

Fig. A.24. *From top to bottom*: the integrated spectrum of NGC 5281 corrected for $E(B-V) = 0.30$, the Yc template spectrum of 20 Myr, the cluster spectrum corrected for $E(B-V) = 0.20$, the Yd template spectrum of 40 Myr, and the corresponding flux residuals between both comparisons. Units as in Fig. 1.

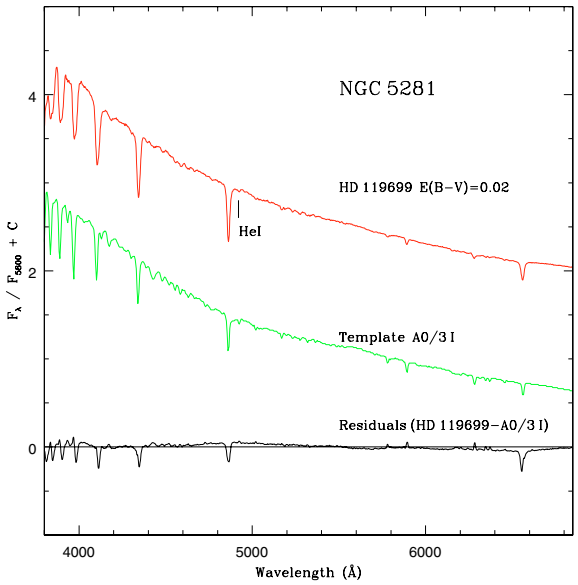

Fig. A.25. Individual spectrum of the bright star HD 119699 of NGC 5281 corrected for reddening (*top*), the SC92 template spectrum which best matches it (*middle*), and the flux residuals according to $(F_{\rm cluster} - F_{\rm template})/F_{\rm cluster}$ (*bottom*). Units as in Fig. 1.

Figure A.24 displays the integrated cluster spectrum corrected for $E(B-V) = 0.30$, compared with the Yc template of 20 Myr. The comparison is quite good as far as the continuum distribution is concerned but it is barely acceptable if we consider the 4000 Å break. It is evident that there are significant differences between both spectra in the depth of the Balmer lines. Such differences, in a somewhat slighter way, are also present when other spectral features are compared, for example the HeI 4921 Å line, which is not in the template. An alternative match with the Yd template of 40 Myr shows better agreement in the depth of the Balmer lines and in the 4000 Å break. Besides, the HeI 4921 Å line, which does not appear in the template Yc, can be seen in template Yd. However, in this older template the K CaII line is barely detectable, which is not the case in the spectrum of NGC 5281. The differences in the Balmer lines in both comparisons may be due to the fact that the cluster spectrum is almost dominated by the bright A-type supergiant HD 119699. Consequently, both comparisons indicate an intermediate age of 30 Myr and hence an intermediate reddening $E(B-V) = 0.25$. Since the Balmer lines also suggest an intermediate age between the the Yc and Yd templates, we adopted an age of 30 ± 10 Myr for NGC 5281. The reddening-corrected spectrum of NGC 5281, averaged with those of Hogg 10 and Trumpler 21, was used to define a new open cluster template of 30 Myr (Sect. 5.2).

The peculiarly elongated stellar distribution of NGC 5281 allowed us to obtain individual extractions of some bright stars, avoiding contamination by neighbouring stars. In Fig. A.25, the reddening-corrected spectrum of HD 119699 is compared with the A0/3 I template of SC92. Although there is good agreement between both spectra, the Balmer lines show that HD 119699 could be a little later than the template. Note that even the weak HeI 4921 Å line is visible in both spectra. The low reddening found for HD 119699 may be due to the discreteness of the SC92 library, as far as the separation of spectral types is concerned. The spectral type A2 II assigned to HD 119699 in the Stephenson & Sanduleak (1971) catalogue is compatible with the comparison made in this work.

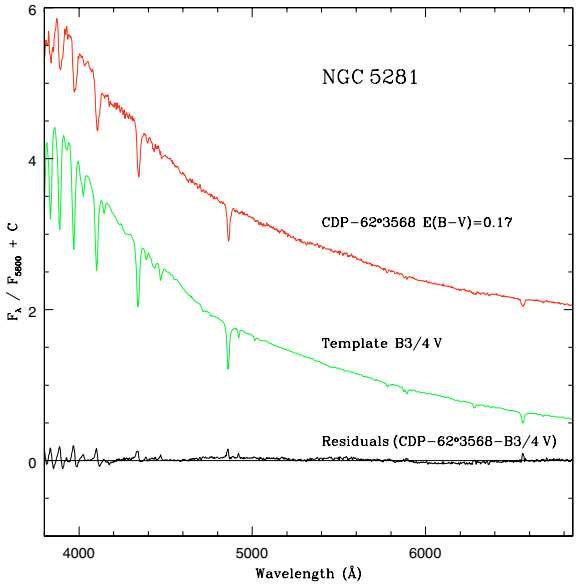

Fig. A.26. Individual spectrum of the bright star CPD-62°3568 of NGC 5281 corrected for reddening (*top*), the SC92 template spectrum which best matches it (*middle*), and the flux residuals according to $(F_{\rm cluster} - F_{\rm template})/F_{\rm cluster}$ (*bottom*). Units as in Fig. 1.

Figure A.26 shows the comparison of the reddening-corrected spectrum of star CPD -62°3568 (No. 2 from MV73, $V = 8.80$), with the B3/4 V template from SC92. This spectral type is consistent with the position of this star in the MV73 *UBV* diagrams, whereas the reddening derived here enables us to confirm its cluster membership status. In Fig. A.27 the reddening-corrected spectrum of HD 119682 (No. 3 from MV73, $V = 7.98$) is compared to the B1 I template from the same library. The strong emission observed in H_α and H_β in the spectrum of HD 119682 are consistent with the spectral type OB^+ce,1e reported in Stephenson & Sanduleak (1971). HD 119682 is undoubtedly a Be supergiant cluster member. Finally, in Fig. A.28 we compare the individual spectrum of the

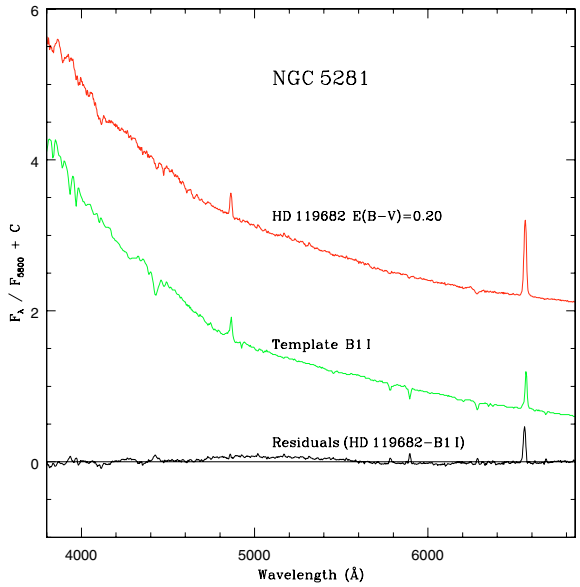

Fig. A.27. Individual spectrum of the star HD 119682 of NGC 5281 corrected for reddening (*top*), the SC92 template spectrum which best matches it (*middle*), and the flux residuals according to $(F_{\rm cluster} - F_{\rm template})/F_{\rm cluster}$ (*bottom*). Units as in Fig. 1.

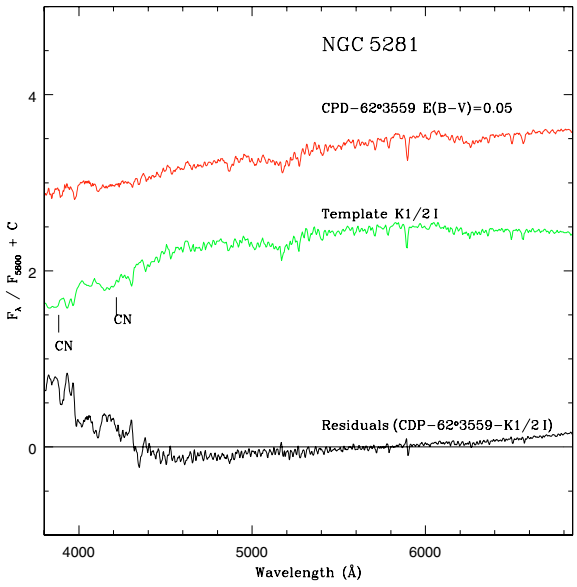

Fig. A.28. Individual spectrum of the star CPD-62°3559 of NGC 5281 corrected for reddening (*top*), the SC92 template spectrum which best matches it (*middle*), and the flux residuals according to $(F_{\rm cluster} - F_{\rm template})/F_{\rm cluster}$ (*bottom*). Units as in Fig. 1.

late-type star CPD -62°3559 (No. 11 from MV73, $V = 8.39$), corrected for reddening, with the K1/2 I template from SC92. Both the star and template spectra show excellent agreement provided that we only consider the spectral region for $\lambda > 4500$ Å. For $\lambda < 4500$ Å, the differences between both spectra are evident, being more so the CN 4216 Å and 3883 Å bands in the template, while they are scarcely visible in the spectrum of CPD -62°3559. This implies that CPD -62°3559 is probably later than the K1/2 I template from SC92, which is consistent with the spectral type K4 Ib-II assigned by Clariá et al. (1989) based on *DDO* colours. The low reddening value derived for CPD -62°3559 (Fig. A.28) is probably due to the discreteness of the SC92 spectral library.

A.18. Lyngå 1

This is a very small open cluster (diameter <2′), originally identified by Lyngå (1965), lying in the Centaurus OB1 association. Reasonably good matches are found with both the Yf (100 Myr) and Ye (45−75 Myr) templates, with colour excesses $E(B-V) =$ 0.35 and 0.38, respectively (Fig. A.29). The age inferred from Balmer lines supports the comparison with the Yf template. We therefore adopted an age of 100 ± 50 Myr for Lyngå 1, in good agreement with the age derived by Vázquez et al. (2003) from *CCD UBVRI* photometric observations. These authors determined a somewhat larger reddening value, namely $E(B-V) =$ 0.45. It is probable, however, that the difference between the spectroscopic and photometric reddening values is due to a certain amount of internal dust associated with the cluster. Note in Fig. A.29 the presence of an unexpected CaI 6493 Å line. Such a line could be of interstellar origin or else it could come from an evolved cluster star. The reddening-corrected spectrum of star No. 1 from Vázquez et al. (2003), compared with the SC92 K1/2 I template, is shown in Fig. A.30. This comparison supports the conclusion that the above-mentioned star is a red supergiant cluster member. This conclusion is not in agreement with that reached by Peterson & Fitzgerald (1988); it is, however, consistent with that of Vázquez et al. (2003).

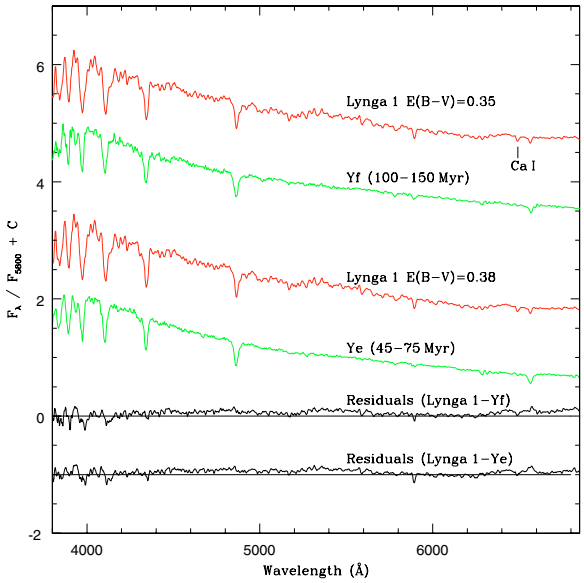

Fig. A.29. *From top to bottom*: the integrated spectrum of Lyngå 1 corrected for $E(B-V) = 0.35$, the Yf template spectrum of (100−150) Myr, the cluster spectrum corrected for $E(B-V) = 0.38$, the Ye template spectrum of (45−75) Myr, and the corresponding flux residuals between both comparisons. Units as in Fig. 1.

A.19. Pismis 20

Also known as BH 170 (van den Bergh & Hagen 1975), Pismis 20 was first recognised as an open cluster by Pismis (1959). This is a distant, compact, young group of stars located in the heart of the Circinus OB1 association. A detailed *CCD UBVRI* photometric study of Pismis 20 was carried out by Vázquez et al. (1995), who derived $E(B-V) = 1.24$ and an age of 5 ± 1 Myr. There are a number of WR stars present in the cluster (Lundstrom & Stenholm 1984), among them star WR 67, whose spectral type is WN6 (van der Hucht et al. 1981). This star as well as the B2 Ia-O star HD 134959, are very likely cluster

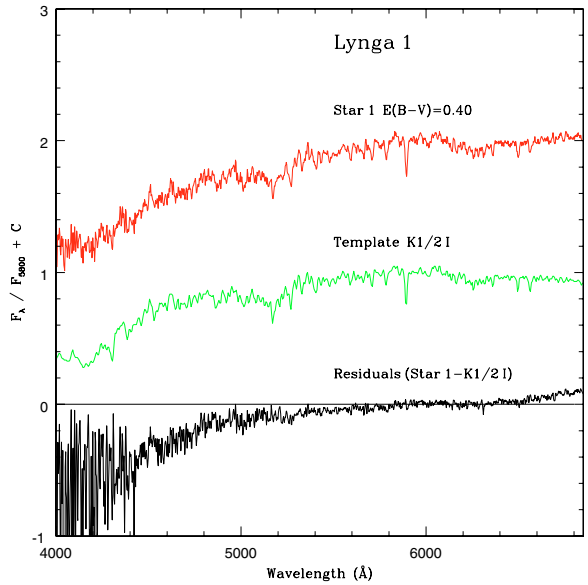

Fig. A.30. Individual spectrum of the star No. 1 from Vázquez et al. (2003) of Lyngå 1 corrected for reddening (*top*), the SC92 template spectrum which best matches it (*middle*), and the flux residuals according to $(F_{\rm cluster} - F_{\rm template})/F_{\rm cluster}$ (*bottom*). Units as in Fig. 1.

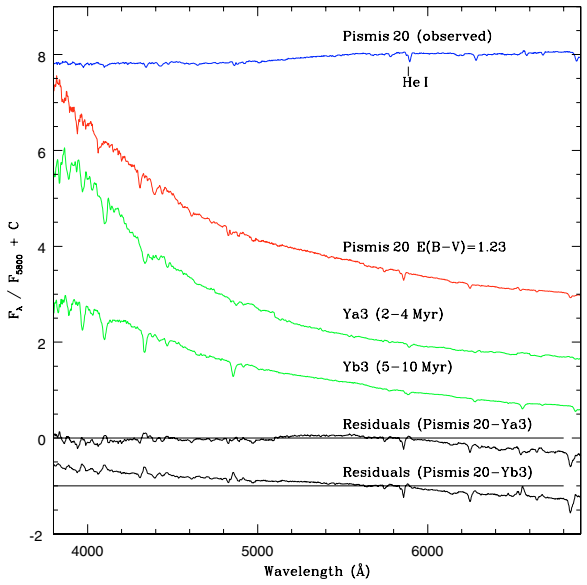

Fig. A.31. *From top to bottom*: the observed integrated spectrum of Pismis 20, the cluster spectrum corrected for the derived $E(B-V)$ value, the Ya3 (2−4 Myr) and Yb3 (5−10 Myr) template spectra, and the corresponding flux residuals between both comparisons. Units as in Fig. 1.

members (Sagar et al. 2001). Notice the extreme reddening effects in the observed spectrum of Pismis 20 (Fig. A.31). We also show in Fig. A.31 the spectrum corrected for $E(B-V) = 1.23$ and the template Ya3 (2−4 Myr) which best matches it. However, there are several features seen in the Pismis 20 spectrum – in the region near Hβ, for example – which are not observed in this template. We conclude that Pismis 20 must be slightly older than the Ya3 template. In Fig. A.31 we show an alternative comparison with Yb3 template of (5−10) Myr. Note that the HeI 5876 Å line is apparent in both templates. Our adopted final values (Table 4) are in excellent agreement with those derived by Vázquez et al. (1995). In Fig. A.32 we compare the individual spectrum of star HD 134959, corrected for $E(B-V) = 1.12$, with the SC92 B3/5 I and B1 I templates. Apart from the circumstellar emission present in the B1 I template, the reddening-corrected spectrum of HD 134959 confirms the findings of Sagar et al. (2001) in the sense that this is certainly a B-type supergiant cluster member.

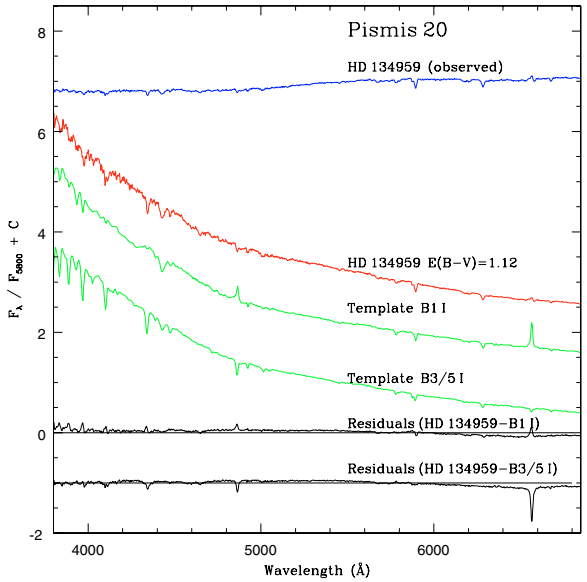

Fig. A.32. *From top to bottom*: the observed individual spectrum of the star HD 134959 of Pismis 20, the star spectrum corrected for reddening, the SC92 B1 I and B3/5 I template spectra, and the corresponding flux residuals between both comparisons. Units as in Fig. 1.

A.20. Hogg 22

This object, first recognised as an open cluster by Hogg (1965a,b), is a poor and scarcely concentrated group of stars in Carina dominated by the bright star HD 150958 ($V = 7.29$), previously classified as O6ek by Whiteoak (1963). As shown in Fig. A.33, the cluster integrated spectrum (without the contribution of the brightest star HD 150958), corrected for $E(B-V) = 0.55$, exhibits very good agreement with the Yb1 template (5−10 Myr). As can be seen in this figure, the same cluster spectrum, corrected for $E(B-V) = 0.75$, also compares reasonably well with the Ya3 template (2−4 Myr). Depending on what spectral features are examined, both comparisons look reasonable enough. For example, the Balmer lines better fit those of the oldest template (Yb1), while the observed continuum better matches the younger template (Ya3). The presence of HeI and HeII lines in the spectrum of Hogg 22 are compatible with the cluster being of an age in between the two mentioned templates. So we adopted for the cluster an age of 4.5 ± 2.0 (Table 4). Notice that the age adopted is compatible with the one indicated by the EWs of the Balmer lines.

Based on *UBV* photoelectric photometry of 10 bright stars in the cluster field, MV73 showed the interstellar reddening in front of Hogg 22 to be variable, the mean value being $\langle E(B-V)\rangle = 0.66$. According to these authors, the earliest photometric spectral type in Hogg 22 is O9. More recently, Kharchenko et al. (2005) reported $E(B-V) = 0.65$ and an age of 5 Myr for Hogg 22, in good agreement with the findings of MV73. The reddening value reported by them practically coincides with the mean $E(B-V)$ value determined through the template matches. The integrated spectrum of Hogg 22 – without the contribution of the bright star HD 150958 – exhibits the typical features of an

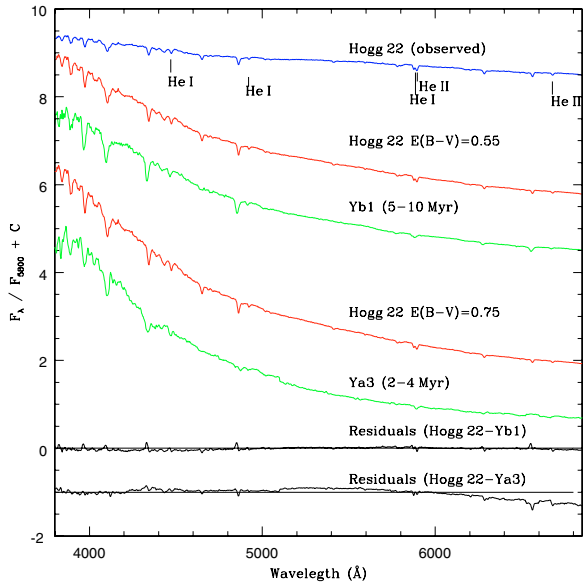

Fig. A.33. *From top to bottom*: the observed integrated spectrum of Hogg 22 (without the contribution of the brightest star HD 150958), the cluster spectrum corrected for $E(B-V) = 0.55$, the Yb1 template spectrum of (5−10) Myr, the cluster spectrum corrected for $E(B-V) = 0.75$, the Ya3 template spectrum of (2−4) Myr, and the corresponding flux residuals between both comparisons. Units as in Fig. 1.

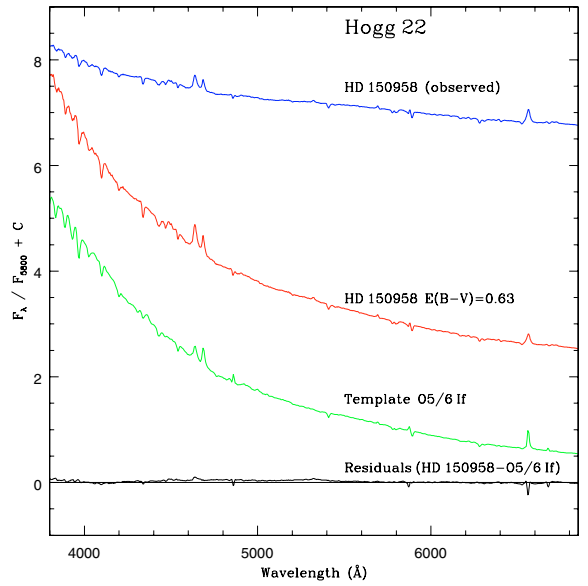

Fig. A.34. *From top to bottom*: the observed individual spectrum of the star HD 150958 of Hogg 22, the spectrum corrected for reddening, the SC92 template spectrum which best matches it, and the flux residuals according to $(F_{\rm cluster} - F_{\rm template})/F_{\rm cluster}$. Units as in Fig. 1.

intermediate spectrum between the Ya and Yb templates from Piatti et al. (2002).

The reddening-corrected spectrum of HD 150958 compares remarkably well with the SC92 O5/6 If template (Fig. A.34). Consequently, this object is very likely a blue supergiant cluster member. This star – No. 1 from MV73 and classified as O6ek – has a photometric reddening of 0.64 mag, which is similar to the one determined here.

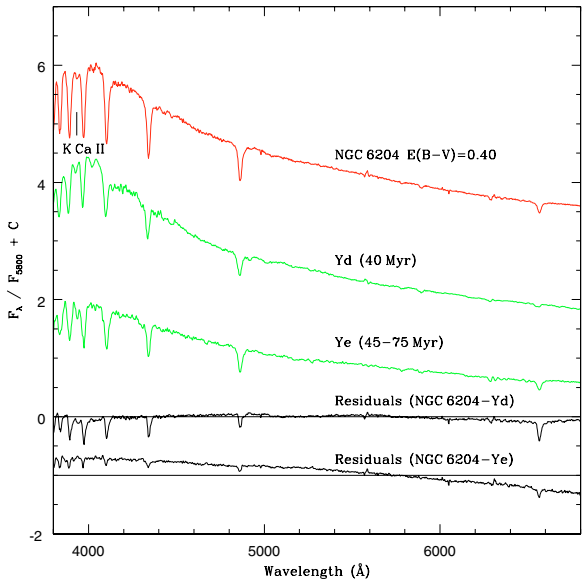

Fig. A.35. *From top to bottom*: the integrated spectrum of NGC 6204 corrected for the derived $E(B-V)$ value, the Yd (40 Myr) and Ye (45−75) Myr template spectra, and the corresponding flux residuals between both comparisons. Units as in Fig. 1.

A.21. NGC 6204

This is also a very compact open cluster, also referred to as Cr 312 (Collinder 1931) or BH 196 (van den Bergh & Hagen 1975), which was classified as I3m by AH03. Based on *UBV* photoelectric photometry of 13 stars, MV73 derived $E(B-V) = 0.39$. More recently, however, Carraro & Munari (2004) derived $E(B-V) = 0.47$ and an age of 80 Myr from a multicolour *CCD* photometric study. The Balmer lines in the cluster integrated spectrum indicate an age between 40 and 60 Myr, while the best comparison of the observed integrated spectrum is obtained with the Yd template (40 Myr), using $E(B-V) = 0.40$ (Fig. A.35). In particular, K CaII line suggests this same age, which is slightly lower than that derived by Carraro & Munari (2004). The resulting reddening value is also a little lower than that determined by the above authors. The difference between both $E(B-V)$ colour excesses can be explained if we consider the fact that the integrated spectrum allows us to determine the reddening produced by the material in front of the cluster (excluding internal dust absorption). Since the Balmer lines in the cluster spectrum, somewhat deeper than those in the template, better resemble those of the Ye template of 45−75 Myr (Fig. A.35), we adopted for NGC 6204 an age of 60 ± 10 Myr (Table 4).

A.22. Pismis 24

Pismis 24, also known as BH 227 (van den Bergh & Hagen 1975), was first recognised as an open cluster in Scorpius by Pismis (1959). The cluster is embedded in the HII region NGC 6357. The blue DSS image of Pismis 24 shows a 20″ sized object of unknown type just east of Pismis 24, catalogued as the nonstellar object GSC 07383-00677. This object, however, is probably some foreign material that was on the DSS, as it does not appear in the red DSS image. MV73 measured photoelectrically in the *UBV* system 15 stars in the cluster field, 12 of which they concluded to be members. They derived a distance of 2.09 kpc and a mean colour excess $\langle E(B-V)\rangle = 1.72$, being O7 the earliest spectral type.

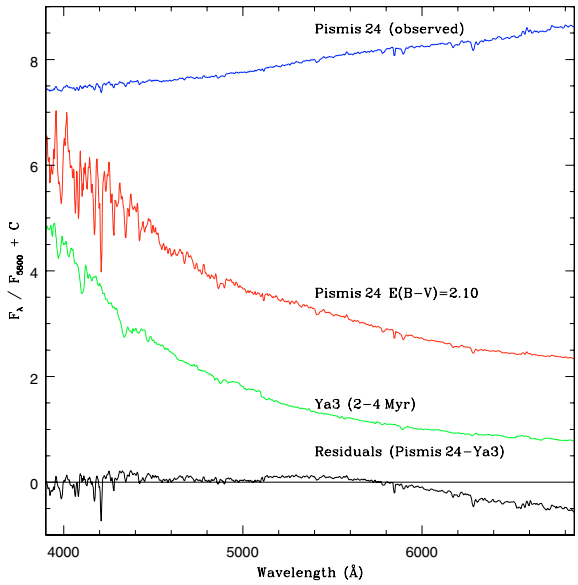

Fig. A.36. *From top to bottom*: the observed integrated spectrum of Pismis 24, the cluster spectrum corrected for $E(B-V) = 1.20$, the Ya3 template spectrum of (2−4) Myr and the flux residuals according to $(F_{\rm cluster} - F_{\rm template})/F_{\rm cluster}$. Units as in Fig. 1.

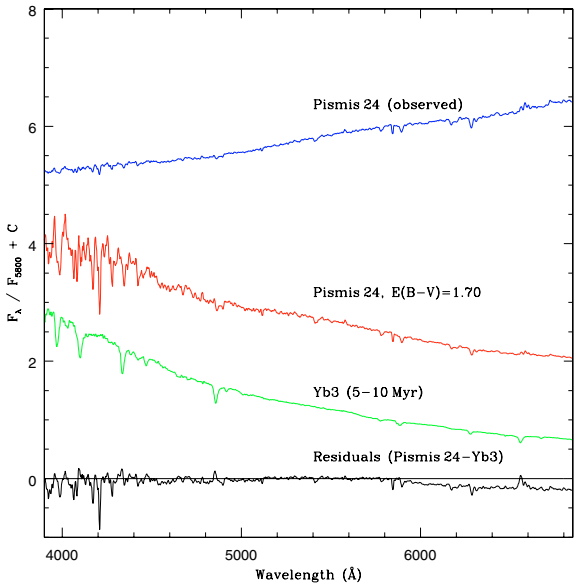

Fig. A.37. *From top to bottom*: the observed spectrum of Pismis 24, the cluster spectrum corrected for $E(B-V) = 1.70$, the Yb3 template spectrum of (5−10) Myr, and the flux residuals according to $(F_{\rm cluster} - F_{\rm template})/F_{\rm cluster}$. Units as in Fig. 1.

More recently, Massey et al. (2001) classified HDE 319718 ($V = 10.43$), the brightest star in the cluster field, as a new O3 If star. O3 type stars are very rare, with only five possible examples known in the Milky Way (Walborn 1994; Massey & Johnson 1993). Since the O3 spectral type represents the hottest spectral class, HDE 319718 must be of extremely high mass. Pismis 24 also contains the WR star HD 157504 (WR 93), of type WC7 (Massey et al. 2001). The EWs of the Balmer lines in the integrated cluster spectrum (Table 3) clearly indicate that Pismis 24 is very young. The cluster spectrum has a low S/N ratio for $\lambda < 4400$ Å. In Fig. A.36 the reddening-corrected spectrum of Pismis 24 compares fairly well with the Ya3 template of (2−4) Myr. It can be observed, however, that the template spectrum has practically no lines in this spectral region, while several weak lines can be seen in the cluster spectrum. An alternative match with Yb3 template of (5−10) Myr, using $E(B-V) = 1.70$ (Fig. A.37), also yields an acceptable agreement. The similarity between the presence and depth of the spectral lines for $\lambda > 4800$ Å is noticeable in this case. It is for this reason that we adopted for Pismis 24 an intermediate age of 5 ± 3 Myr and $E(B-V) = 1.90 \pm 0.05$. Therefore, Pismis 24 turns out to be the most reddened cluster of the present sample. The resulting age agrees with that reported by Massey et al. (2001).